

A WAVELET-BASED FEATURE EXTRACTION TECHNIQUE FOR PARTIAL IRIS RECOGNITION

Md. Rabiul Islam

**A thesis submitted in fulfilment of the requirements for the degree of Master of Science
in Computer Science**

Faculty of Computer Science and Information Technology

UNIVERSITI MALAYSIA SARAWAK

2011

Dedication

To my parents, Nanima, Mama and my beloved wife, Asma Khatun – your love, care, prayers and support have been my great inspiration and have endured me through all the difficult times.

Acknowledgements

I would like to extend sincere appreciation to my supervisor, Professor Dr. Wang Yin Chai, for his patient supervision and encouragement throughout this research. I thank him for providing me with helpful ideas, guidance, comments, criticisms, facilities and support for the research. I would like to convey my special thanks to Professor John Daugman for his valuable conference and journal papers and discussion. I would like to express my appreciation to the Chinese Academy of Sciences' Institute of Automation (CASIA) for generously providing the iris image database.

I appreciate the Faculty of Computer Science and Information Technology for the high quality education and the research facilities I received. The faculty lab has always been a stimulating environment for conducting research. I thank all the technical, administrative and academic staff of the faculty.

I thank my fellow researchers Asma Khatun, Lee Guang Heng, Lee Beng Yong, Liew Lee Hung, and Voon Buang Hong for providing a friendly research environment and technical discussions.

I thank my family members specially my parents and uncle Md. Hamidul Islam for their unending encouragement and support.

Lastly, to Centre for Graduate Studies, Universiti Malaysia Sarawak for the Postgraduate Scholarships and for giving me the opportunity to pursue my research leading to masters degree.

Abstract

(Feature extraction is an important task in the overall processing of iris biometric in an iris based biometric authentication system. The existing approaches are using complete iris image to extract iris features. But, it is difficult to get complete iris images for feature extraction because a person's eyes are naturally covered by the eyelids and eyelashes. Thus, the correct recognition rate decreased in the existing approaches due to occluded eyelids and eyelashes classified as an iris region.

Therefore, this research proposed an iris image model and a feature extraction method for partial iris recognition. Several issues that are investigated in this research i.e. which parts or regions of the iris are more stable and provide distinctive texture patterns, what is the optimum coverage area of the iris that is required to extract discriminant texture features for partial iris recognition, the existing feature extraction methods and the nature of features whether they can be used for partial iris recognition.)

Daubechies DB8 discrete wavelet transform is generated to extract discriminating texture features of the partial iris image which gives better performance in iris image texture analysis as compared to other methods used in the existing approaches. The three different kinds of partial iris image models have been proposed and designed to identify the significant part of the iris for feature extraction of the partial iris image. Daubechies DB8 discrete wavelet transform is repeatedly performed to the normalized partial iris image and it decomposes a signal into low-pass and high-pass information in different resolution levels. The three different characteristics vector have been formed with the extracted high frequency components of the wavelet transformed partial iris image of each individual's eye image. This research also highlighted a sign quantization technique that explains how the

characteristics vector is encoded into binary feature vector for unique binary feature vector representation and it gives a computationally effective feature vector which is comprised with only 540 bits.

The proposed feature extraction method for partial iris recognition has been tested with CASIA iris image database. The intra-class and inter-class comparisons have been performed based on Hamming distance similarity measurement technique among the feature vectors generated from the partial iris image of individual's eye image available in the database. The intra-class and inter-class comparisons results demonstrate that distinctive texture features are identified in the inner-right and inner-left sub image of the collarette boundary of the iris. The experiments have been conducted in verification mode in order to measure the accuracy of the proposed method. In the verification mode, the False Accept Rate (FAR) 3.23% and False Reject Rate (FRR) = 3.5% and Equal Error Rate (EER) 0.28% is obtained at a certain threshold. The correct verification rate (CVR) is calculated from the obtained FAR and FRR. The remarkable correct verification rate (CVR) 93.27% is achieved in this research that is comparable with the existing methods although the partial iris image has been used in this research for feature extraction.

Abstrak

Ekstraksi ciri-ciri merupakan tugas penting dalam pemrosesan keseluruhan iris mata bagi tujuan pengesanan biometric. Pendekatan terkini yang sedia ada perlu menggunakan gambar iris mata yang lengkap untuk ekstraksi ciri-ciri dari iris mata.

Namun, ianya adalah sukar untuk mendapatkan gambar iris yang lengkap untuk ekstraksi ciri-ciri kerana mata seseorang biasanya adalah tertutup oleh kelopak mata dan bulu mata. Jadi, tahap pengenalan yang benar berkurangan dalam pendekatan yang sedia ada kerana kelopak mata dan bulu mata melindungi kawasan mata yang dikelaskan sebagai wilayah iris.

Oleh kerana itu, kajian ini mencadangkan suatu model gambar iris dan kaedah ekstraksi ciri-ciri untuk pengenalan iris separa. Beberapa isu yang telah diteliti dalam penyelidikan ini adalah, bahagian manakah di alam iris adalah lebih stabil dan memberikan pola tekstur yang khas, bahagian manakah yang merupakan bahagian liputan optimum iris yang diperlukan untuk ekstraksi ciri tekstur yang paling diskriminan untuk pengenalan iris separa, dan sejauh manakah ciri-ciri dan kaedah ekstraksi yang sedia ada dapat digunakan untuk pengenalan iris separa.

Transformasi Daubechies DB8 discrete wavelet adalah dihasilkan untuk ekstraksi ciri-ciri tekstur diskriminan dari gambar iris mata separa yang menghasikan prestasi yang lebih baik dalam penganalisan tekstur gambar iris berbanding dengan kaedah lain yang digunakan dalam pendekatan yang sedia ada. Tiga model citra iris separa yang berbeza telah dicadangkan dan direka untuk mengenal pasti bahagian penting dari iris untuk ekstraksi ciri-ciri dari gambar iris separa. Transformasi Daubechies DB8 discrete wavelet diulangi beberapa kali bagi tujuan normalisasi gambar iris separa dan ianya menyebabkan isyarat terurai ke informasi low-pass dan high-pass pada resolusi yang berbeza. Tiga vektor yang

berbeza ciri telah dibentuk dengan komponen frekuensi tinggi yang dihasilkan dari proses transformasi wavelet pada setiap gambar iris mata separa individu masing-masing. Penyelidikan ini juga menyerlahkan satu teknik sign quantization yang menjelaskan bagaimana vektor tersebut diterjemahkan ke ciri-ciri binari untuk tujuan perwakilan unik sambil menghasilkan suatu vektor ciri pengkomputeran yang berkesan yang terdiri hanya dengan 540 bit.

Kaedah ekstraksi ciri yang dicadangkan untuk pengenalan iris separa telah diuji dengan database gambar-gamabr iris CASIA. Perbandingan intra-kelas dan inter-kelas telah dilakukan berdasarkan pengukuran jarak persamaan Hamming antara vektor ciri-ciri yang dihasilkan dari gambar-gambar iris mata separa individu-individu yang sedia di dalam database tersebut. Hasil perbandingan keputusan pengukuran intra-kelas dan inter-kelas ini menunjukkan bahawa ciri tekstur yang distictive boleh dikenalpasti pada bahagian dalaman kanan dan bahagian dalaman kiri batas collarette iris mata.

Eksperimen telah dijalankan dalam mod pengesahan bagi mengukur ketepatan kaedah yang dicadangkan. Dalam mod pengesahan ini, Kadar Penerimaan Salah (FAR) = 3.23% dan Kadar Penolakan Salah (FRR) = 3.5% dan Kadar Salah Sama (EER) = 0.28% telah diperolehi pada ambang batas tertentu. Kadar pengesahan benar (CVR) adalah dikira dengan menggunakan FAR dan FRR tersebut. Kadar pengesahan benar (CVR) yang dicapai dalam kajian ini adalah setinggi 93.27%. Keputusannya adalah setanding dengan kaedah-kaedah kini yang sedia ada meskipun gambar iris separa sahaja yang telah digunakan dalam kajian ini untuk ekstraksi ciri-ciri.

Table of Contents

Dedication.....	ii
Acknowledgements.....	iii
Abstract.....	iv
Abstrak.....	vi
List of Figures.....	xi
List of Tables.....	xiii
List of Abbreviations.....	xiv
CHAPTER 1 INTRODUCTION.....	1
1.1 Background.....	1
1.2 Problem Description.....	6
1.3 Objectives.....	10
1.4 Scope of Study.....	11
1.5 Research Questions.....	12
1.6 Research Methodology.....	13
1.6.1 Literature Review.....	13
1.6.2 Requirement & Specifications.....	14
1.6.3 Designing Proposed Algorithms.....	14
1.6.4 Experiments and Analysis.....	15
1.7 Outline of the Dissertation.....	16
1.8 Summary.....	17

CHAPTER 2 BACKGROUND & SURVEY	18
2.1 Introduction.....	18
2.2 Components of Partial Iris Recognition System	18
2.3 Feature Extraction Techniques.....	20
2.3.1 The Phase Based Method	22
2.3.2 Zero-Crossing Representation Based Method.....	26
2.3.3 Texture Analysis Based Method.....	27
2.3.4 Other Algorithms	36
2.4 Similarity Measurement Techniques.....	39
2.4.1 Hamming Distance.....	39
2.4.2 Normalized Correlation.....	40
2.4.3 Weighted Euclidean Distance.....	40
2.4.4 Nearest Center Classifier.....	41
2.5 Summary	42
CHAPTER 3 PARTIAL IRIS IMAGE REQUIREMENT & FEATURE EXTRACTION FOR PARTIAL IRIS RECOGNITION.....	43
3.1 Introduction.....	43
3.2 Partial Iris Image Requirement	45
3.2.1 Extracting Spatial Partial Iris Image	50
3.3 Feature Extraction of the Partial Iris Image.....	57
3.3.1 Characteristics Vector Generation	67

3.3.2 Binary Feature Vector Representation	70
3.4 Feature Matching and Distance Measure.....	73
3.5 Evaluation Methods.....	74
3.6 Summary	75
CHAPTER 4 EXPERIMENTS AND RESULTS ANALYSIS	77
4.1 Introduction.....	77
4.2 The Sample Database	78
4.3 Performance Evaluation of the Feature Extraction Method for Partial Iris Image Recognition.....	80
4.4 Summary	99
CHAPTER 5 CONCLUSION	101
5.1 Introduction.....	101
5.2 Research Findings and Contributions.....	102
5.3 Limitations	106
5.4 Future Works.....	106
5.5 Conclusion	108
Bibliography.....	110
Appendix I.....	118

List of Figures

Figure 1.1 The typical components of an eye image	2
Figure 1.2 (a), (b), and (c) Example of false acceptance and false rejection due to occlusion of iris image	8
Figure 2.1 Components diagram of the proposed partial iris recognition system.....	19
Figure 2.2 (a) and (b) even- symmetric and odd symmetric wavelet profiles together with their contour plots (adopted from Daugman (1994)).....	23
Figure 2.3 Daugman phase demodulation process (adopted from Daugman (2004)).....	25
Figure 2.4 Zero-crossing of WT (adopted from Boles & Boashash (1998))	27
Figure 2.5 Multiscale representation for iris pattern (adopted from Wildes <i>et al.</i> (1996))...	29
Figure 2.6 (a) Spatial filter with $\delta_x = \delta_y$ (b) spatial filter with $\delta_x > \delta_y$ (c) Gabor filter (d), (e), and (f) are the Fourier spectra of (a), (b), and (c) (image taken from Ma <i>et al.</i> (2003))	32
Figure 2.7 Haar mother wavelet (image taken from Lim <i>et al.</i> (2001))	33
Figure 2.8 Collarette area is occluded by eyelids and eyelashes which are not recognized as correct by the proposed methods of Poursaberi & Araabi (2007).....	35
Figure 3.1 Collarette boundary of the iris	46
Figure 3.2 Proposed partial iris model.....	46
Figure 3.3 Outline of polar transformation process.....	52
Figure 3.4 (a) The original eye image (b) inner right and left model (c) outer right and left model (d) upper and lower model.....	53
Figure 3.5 Extracted & normalized iris images for the three different kinds of partial iris image models.....	56
Figure 3.6 Enhanced iris images for the three different kinds of partial iris image models ..	57

Figure 3.7	A 4-level wavelet decomposition procedure using DB8 wavelets	64
Figure 3.8	The extracted characteristics values distribution of a partial iris image	71
Figure 3.9	(a) Feature vector with 540 bits for inner right and left partial iris image model (b) feature vector with 576 bits for outer right and outer left partial iris image model...	72
Figure 4.1	Iris samples from CASIA iris image databases (a) iris image taken from the first session for training (b) iris image taken from the second session for testing	79
Figure 4.2	Distribution of intra-class and inter-class distances for the templates extracted from the inner right and inner left partial iris image models	82
Figure 4.3	Distribution of intra-class and inter-class distances for the templates extracted from the outer right and outer left partial iris image model.....	87
Figure 4.4	Distribution of intra-class and inter-class distances for the templates extracted from the upper and lower partial iris image model.	89
Figure 4.5	Distribution of intra-class and inter-class distances for the templates extracted from the inner right and inner left partial iris image model from comparing images taken at different session.....	91
Figure 4.6	FAR and FRR for different threshold (HD) values	96

List of Tables

Table I The comparison among the existing methods	37
Table II The low-pass and high-pass filters of DB8.....	65
Table III Intra-class comparisons for images taken at the same session	81
Table IV Inter-class comparisons for images taken at the same session	81
Table V Intra-class comparisons for images taken at the different session	81
Table VI Inter-class comparisons for images taken at the different session.....	81
Table VII Illustration of a subject iris code (028_1_1) Hamming Distance.....	84
Table VIII Illustration of subject's iris code (003_1_3, 008_1_3, 014_1_1, 012_1_2, 015_1_2, 018_1_3, 022_1_1, 023_1_3, 026_1_1, 028_1_1, 029_1_1) Hamming Distance	92
Table IX Performance comparisons of several methods for iris verification	97

List of Abbreviations

FA	False Acceptance
FR	False Rejection
FAR	False Accept Rate
FRR	False Reject Rate
EER	Equal Error Rate
CVR	Correct Verification Rate
HD	Hamming Distance
WED	Weighted Euclidean Distance
DWT	Discrete Wavelet Transform
LPF	Low Pass Filter
HPF	High Pass Filter
DT	Decision Threshold
WT	Wavelet Transform

Chapter 1 Introduction

1.1 Background

Nowadays, it is a common sight to see technology being integrated with the security system that exploits biometrics for application to the identification and verification of individuals for controlling access to secured areas or materials. Biometrics pertains to the use of automated methods for unique human recognition based upon one or more intrinsic physical or behavioral traits (Jain *et al.*, 2004). Physical biological biometrics is the most widely used biometric traits and include unique physical traits of the human body such as fingerprints, iris patterns, facial features, hand geometries, palm prints, retinas, vein structures, etc. (Prabhakar *et al.*, 2003; Jain *et al.*, 2004). Behavioral biometrics include characteristics such as hand-written signature, keystroke dynamics, gait, voice, typing pattern etc. (Prabhakar *et al.*, 2003; Jain *et al.*, 2004). Among all these biometric traits, the iris is established to be the most authentic and accurate (Daugman, 1993) due to its extremely data-rich physical structure, regular features and provide a geometric pattern (Flom & Safir, 1987). The texture of the iris is stabilized when a baby reaches twelve months of age and there are no subsequent changes in the lifetime because it is neither duplicable nor imitable. These are highly randomized appearances of the iris make up for its biometric use.

The iris biometric system is an important to extract distinct iris feature from a given eye image. The iris is an annular part between the pupil and the white sclera. The typical components of an eye image are shown in Figure 1.1.

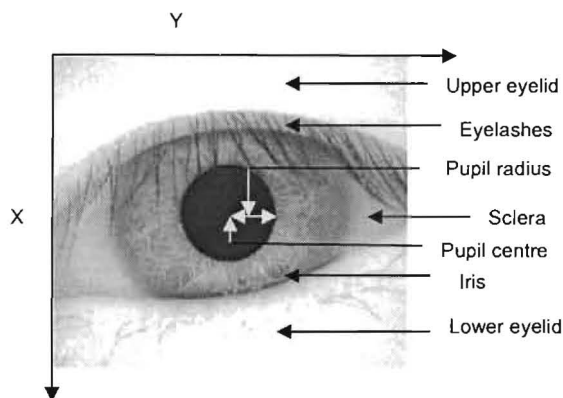


Figure 1.1 The typical components of an eye image

The externally visible surface of the multi-layered iris contains two zones, which often differs in color. An outer ciliary zone and pupillary zone, and these two zones are divided by the collarette which appears in a zigzag pattern (Adler, 1965). The iris part has a number of characteristics such as freckles, corneas, stripe, furrows, crypts, zigzag collarette etc. (Daugman, 1993, 2003; Wildes *et al.*, 1996; Wildes 1997; Ma *et al.*, 2004b), which constitutes what is called as iris features. Those characteristics are converted by the iris recognition system into a code and stored for future verification since iris codes are distinctive for each person, even identical twins have unique irises and even the right and the left iris of a person are different (Basit & Javed, 2007). Human iris recognition process is basically divided into two phases. The phase that deals with the extraction of iris features from an eye image and stores them into database is called the “enrolment process”. The phase that deals with the extraction of iris features a human and compares it with the stored features is called the “matching process” (Dey & Samanta, 2008).

There are several methods in the literature to extract iris features. The methods proposed by Daugman (1993, 1994, 2001a, 2001b, 2003, 2004), Wildes *et al.* (1996), Wildes (1997) and Boles & Boashash (1998), are the best known method among existing schemes for iris recognition. The first commercially adopted algorithm for human authentication was proposed by Daugman (1994). Daugman utilized multiscale Gabor filters to demodulate texture phase structure information of the entire iris. Filtering an iris image with a family of filters resulted in 1024 complex-valued phasors which denote the phase structure of the iris at different scales. Each phasor was then quantized to one of the four quadrants in the complex plane. The resulting 2048-component iris code was used to describe an iris. The similarity between a pair of iris codes was measured by Hamming Distance (HD). The Hamming distance weights all bits in an iris code evenly. However, Hollingsworth *et al.* (2008) reported that not all the bits in an iris code extracted from the entire iris are equally useful since the local region of the iris may be affected by occlusion such as interference of eyelids and eyelashes and other extraneous artifact. Daugman algorithm may produce very promising result in favorable conditions (Gopikrishnan & Santhanam, 2010) but may produce False Accept Rate (FAR) and False Reject Rate (FRR) due to these deformations. The FAR and FRR are two important metrics to measure the accuracy of any biometric based authentication system (Prabhakar *et al.*, 2003; Jain *et al.*, 2004; Anon, 2008). The local region for feature extraction must be small enough in order to achieve high accuracy. Daugman system extracted feature from the entire iris and proposed a high dimensional feature vector with 2048 components that may increase overall processing time of the iris recognition system (Roy & Bhattacharya, 2008).

Wildes *et al.* (1996) and Wildes (1997) employed a two dimensional bandpass decomposition method to extract the distinctive spatial characteristics of the human iris. A Laplacian pyramid

has been used for decomposition the iris texture into four different frequency bands. In order to make a detailed comparison between two iris images it establishes a precise correspondence between characteristics structures across the pair. This matter has been attacked via an area based, image registration technique. With the model and data images accurately and precisely registered, an appropriate match metric can be based on integrating pixel differences over spatial position within each frequency band of the image representation. Normalized correlation has been used to accomplish this notion. The correlations are performed over small block of pixels (8×8) in each spatial frequency band. A goodness of match is derived for each band by combining the block correlation values by the median operation. The Wildes approach made use of more of the available data, by not binarizing the bandpass filtered result, and hence might be capable of finer distinctions; however, it yields a less compact representation and this approach uses a very computationally image registration technique. Although combining the block correlation values by the median operation leads certain robustness against misregistration, however misregistration still is the main reason for false rejection (Ma *et al.*, 2004b). That is, misregistration and occlusion of the iris images may affect the verification accuracy of this method.

Boles & Boashash (1998) proposed a technique to extract and represent the features of the iris by fine-to-coarse approximations at different resolution levels based on the wavelet transform. The dyadic wavelet transform was employed for wavelet decomposition. Zero crossing of the wavelet transform at various levels are calculated over concentric circles on the iris, and the resulting one-dimensional (1-D) signals are compared with model features using different dissimilarity functions. Boles and Boashash (1998) create two dissimilarity functions for the purposes of matching, one using every point of the representation and the other using only the

zero crossing points. The main problem of this method is that the number of zero-crossing can differ among iris image samples of an identical iris due to noises Kim *et al.* (2006).

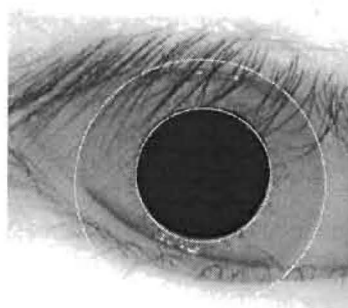
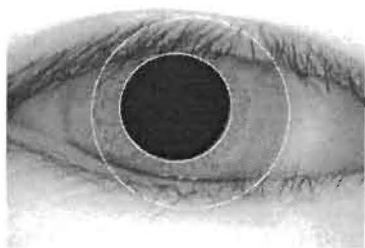
Prior research has assumed that all parts of an entire iris are equally valuable. Instead, some existing approaches claim that parts of the iris are more valuable, but still they use the same portions of the iris for all iris images. From the background survey and analyzing iris images from the well known CASIA iris image database (CASIA-Iris Image Databases Version 1.0 (CASIA-IrisV1)), it is observed that iris part is heavily affected by the occlusion of eyelids and eyelashes (Annapoorani *et al.*, 2010; Yahya & Nordin, 2010), improper eye opening and extraneous artifact in most of the cases (Dey & Samanta, 2008). The current state of the technology used to extract iris features from the whole iris image, which requires storage of excess data and introduces additional sources of errors (Anon, 2006). However, the occlusion of eyelids and eyelashes of the iris region are noise factors that degrade the performance of iris recognition. If the occluded eyelids and eyelashes classified as an iris region, the false iris region information decreases the recognition rate (Min & Park, 2009). This deformation may also alter feature attributes in the feature vector. In such a situation, existing iris image recognition approaches may enhance False Accept Rate (FAR) and False Reject Rate (FRR). Ma *et al.* (2007) found that occlusion of iris images by the eyelids and eyelashes are the main reasons of the failure verification. Hence, it requires empirical analysis in order to determine how different parts of an iris image may be more or less valuable. Bearing all these into account, it is observed that iris image recognition system requires a cooperative subject to overcome the situation while False Accept Rate (FAR) and False Reject Rate (FRR) take place due to partially occluded iris images. Hence, this research aimed to identify a person by their only significant portion of the iris i.e. quite safe from the previously mentioned distortion and demonstrate high discriminability among the different iris images in the

database. Existing feature extraction methods mainly extract features from the complete iris and may not be fitting for extracting features from the only significant portion of the iris or partial iris image. It is required to generate a feature extraction method that extract features from the partial iris image and capable of producing high discriminant features. The proposed feature extraction method of the partial iris image would be very efficient in designing iris recognition system where capturing the entire iris may not be feasible.

1.2 Problem Description

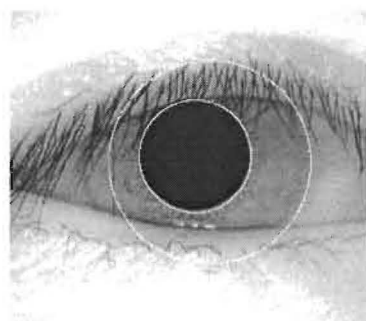
Existing approaches produce false result due to incomplete iris image. The existing approaches are used to extract iris feature from the complete iris. But in practical situation, it is observed that the iris part is partially occluded by interference of eyelids and eyelashes, improper eye opening, light reflection and image quality is degraded because of low contrast image and other man made artifice (Dey & Samanta, 2008). Existing feature extraction methods extract iris features from the complete iris and keep the data into the database as unique feature vector during enrollment for further identification and verification. It is observed that unfortunately $\frac{1}{3}$ of the complete iris is covered by eyelid and some part of the iris is often covered by eyelashes (Wei *et al.*, 2005) in most of the cases during verification/identification due to afore mentioned distortion. Hence, existing approaches produce inaccurate iris identification/verification result due to loss of abundant characteristics information as compared to the once enrolled feature vector. This deformation may alter feature attributes in the feature vector and unfortunately may correlate with the others feature vector in the database and this may cost by occurring false acceptance (FA) and false rejection (FR) during identification/verification in the existing approaches. Figure 1.2 shows some examples of occluded iris images adopted from the CASIA iris image database that occurs

false acceptance and false rejection due to occlusion by eyelids and eyelashes. Figure 1.2 shows the localized pupil and the entire iris boundary and their corresponding unwrapped normalized entire iris image. The existing approaches extract features from the entire normalized iris image to form individually unique feature vector. But, the normalized entire iris image is often obstructed by eyelids and eyelashes and these are classified as iris region as shown in Figure 1.2. If the occluded eyelids and eyelashes are classified as an iris region, the false iris region information decreases the recognition rate (Min & Park, 2009). Ma *et al.* (2004b) reported that if eyelid and eyelash detections are performed with all these existing methods, their respective performance would be slightly improved. Bearing all these into account, it is observed that iris image recognition system requires a cooperative subject to overcome the situation while False Acceptance (FA) and False Rejection (FR) take place due to incomplete iris image. Hence, it is required to design a method in order to identify a person by their only significant portion of the iris or partial iris image i.e. quite safe from the afore mentioned distortion and demonstrate high discriminability among the different iris images.



(a) Localized (top) and
normalized (bottom) iris
image

(b) Localized (top) and
normalized (bottom) iris
image



(c) Localized (top) and normalized (bottom)
iris image

Figure 1.2 (a), (b), and (c) Example of false acceptance and false rejection due to occlusion of iris image

Existing feature extraction methods mainly extract features from the complete iris and may not be fit for extracting features from the only significant portion of the iris or partial iris image. Daugman phase based method (Daugman, 1993, 1994, 2001a, 2001b, 2003, 2004) used Gabor filters to extract phase information by spanning 8-fold range from the complete iris across all of the sampled position set by polar coordinate parameter r and θ in order to encode 2048 bit iris code. But, the outputs of Gabor filter banks are not mutually orthogonal, which may result in a significant correlation between texture features (Unser, 1995). These transformations are usually not reversible, which limits their applicability for texture synthesis (Unser, 1995). Hence, Gabor filters are not suitable to extract discriminant texture features from the partial iris image. In this research, only a significant portion of the iris image is utilized to extract discriminant iris texture features and it is needed to make use of the whole component of the partial iris image to extract unique features. The only phase information of the partial iris image from the sampled position set by polar coordinate parameter r and θ will not provide discriminant texture features for partial iris image recognition. Thus, the Daugman phase based method may not be suitable to extract features from the partial iris image or only significant portion of the iris. Boles & Boashash (1998) proposed a method to extract and represent the features of the iris by fine-to-coarse approximations at different resolution levels based on the dyadic wavelet transform. The number of zero crossing of the wavelet transform at various levels is calculated as features on the complete iris. The problem of this method is that the number of zero-crossing can differ among iris image samples of an identical iris due to noises (Kim *et al.*, 2006). Number of zero crossing will be decreased predominantly in case of partial iris image. The lowest number of zero-crossing information may not be enough to produce discriminant features for partial iris image recognition. Lim *et al.* (2001) employed the Haar wavelet transform to extract features from the iris image region.

However, Haar wavelet functions have disadvantages that the characteristic values are discontinuous and rapidly changes and that high resolution of the images cannot be obtained in a case where the images are again decompressed after they have been compressed (Wang *et al.*, 1998). It is also observed that the numbers of extracted iris features in the existing approaches are very large (>1024 bits) where the higher computations and space are required to process and store these iris features. Hence, it is required to generate a feature extraction method that extracts features from the partial iris image and capable of producing high discriminant features with as few as possible number of features.

1.3 Objectives

The main objective is to design and develop a feature extraction method for partial iris image recognition using Daubechies DB8 discrete wavelet transform. The other specific objectives can be summarized as follows:

- (i) To develop an algorithm in order to extract discriminant texture features with low dimensional feature vector using Daubechies DB8 discrete wavelet transform of the partial iris image.
- (ii) To identify significant part in the collarette boundary of the iris that has most distinguishable patterns and could be used for partial iris image recognition.
- (iii) To analyze the stability and performance of the proposed feature extraction method for partial iris image recognition through intra-class and inter-class comparisons based on Hamming distance similarity measurement technique.

1.4 Scope of Study

The partially occluded iris images are the major problem in the existing feature extraction approaches for iris recognition. Occlusion occurs especially frequent because it is natural for a person's eyes to be covered by the eyelids and eyelashes. Ma *et al.* (2007) found that occlusion of iris images by the eyelids and eyelashes are the main reason of the failure verification. Munemoto *et al.* (2008) stated that it is difficult to properly identify/verify an individual when iris images are partially occluded by the eyelids and eyelashes or other extraneous artifacts. Bremananth & Chitra (2008) reported that 40% of iris images have been obscured by eyelids and eyelashes of which 35% of images hit the iris top portions. Ma *et al.* (2004b) reported that 57.7% of false reject rate (FRR) is incurred by the occlusion of eyelids and eyelashes. Many works in the existing approaches performed eyelids and eyelash detection algorithm. But Ma *et al.* (2004b) stated that if eyelid and eyelash detections are performed with all these existing approaches, their respective performance would be slightly improved. Dong *et al.* (2009) also stated that partially occluded iris images may cause false acceptance during verification/identification. In the LSE identity project interim report (2005) claimed that the number of uncertain bits exceeds a threshold during partial occlusion of iris images and the measurement must be attempted again. If the threshold is set too low there will be too many false matches. Recently, Tajbakhsh *et al.* (2010) also reported that, despite the great progress in iris recognition system, the user friendliness of iris-based recognition system is still a challenging issue and degrades significantly when iris images are affected by degradation factors such as eyelids and eyelashes occlusion. Therefore, this research focuses on designing a feature extraction method for partial iris image recognition in order to identify/verify an individual by their only significant portion of the iris or partial iris image that is quite safe from the above mentioned distortion in most of the cases. Although, there are

numerous feature extraction methods currently available, these methods are being used to extract features from the entire iris image. After analyzing the existing feature extraction methods, it is observed that these methods may not be fit to extract features from the partial iris images. Hence, this research is aimed to design a feature extraction method for partial iris image recognition. This research also proposes several partial iris image models in order to discover the stable region of the iris for partial iris image recognition and these are details described in section 3.2.

1.5 Research Questions

Several feature extraction method that has been used to extract features of the entire iris image was studied. Daugman (1993, 1994, 2001a, 2001b, 2003, 2004) used 2-dimensional Gabor filters to extract the textural information of the iris images. The phase information by spanning 8-fold range from the entire iris set by polar coordinate parameter r and θ were used as unique features. Boles and Boashash (1998) used dyadic wavelet transform to extract unique features. The numbers of zero-crossing information of the decomposed signals were used as unique features. Wildes *et al.* (1996) used Laplacian of Gaussian filters to extract the distinctive features of the iris. Normalized correlation values in each spatial frequency band of filtered image were used as unique features. Ma *et al.* (2003) constructed a bank of spatial filters, whose kernels were used to extract texture features of the iris. The filtered iris image was divided into 8×8 small blocks to extract statistical features. The mean and average absolute deviation value of those blocks were calculated and used as unique features. Lim *et al.* (2001) used Haar wavelet to extract features of the iris. This approach extract iris features corresponding to high pass filter of the wavelet transformed image and used as unique features. Ma *et al.* (2004b) construct a set of one-dimensional intensity signals from the 2-

dimensional normalized iris images. They used a special class of wavelet to represent the resulting 1-D intensity signals. The position sequence of local sharp variations points in such signals were used as unique features. As this research is aimed to explore a feature extraction method for partial iris image recognition, several research questions need to be addressed

- 1) Are the existing feature extraction techniques in iris recognition suitable to extract discriminant texture features of the partial iris image?
- 2) Which parts or regions of the iris is more stable and provides discriminating texture patterns that can be used to extract features for partial iris recognition?
- 3) How to unwrap partial iris image region from the different location of the iris?
- 4) What is the minimum percentage of the visible iris texture patterns that is required to extract discriminant features for partial iris recognition?

1.6 Research Methodology

This research is conducted in a systematic order. The research is carried out starting from literature review to identify the major problems and their potential solutions in existing iris image recognition system. The research continues to discuss on the design proposed to explore a feature extraction method for partial iris image recognition. This method will also be used to identify the stable region on the iris for partial iris image recognition. Experiments and analysis were also conducted to justify the success of this research. Details on the task done in each stage of the research are discussed in following paragraphs:

1.6.1 Literature Review

Reviews are conducted on several areas related to iris image recognition system. These include the review on existing feature extraction methods to identify their problems in iris

image recognition. From the initial review, the problem of using the entire iris image for feature extraction was agreed. Thus, this research is aimed to explore a feature extraction method for partial iris image recognition. In the later part of the literature review, the existing feature extraction method was studied and analyzed whether these method can be used to extract features of the partial iris image. Besides analyzing existing feature extraction methods, other data mining techniques were also reviewed to find a suitable method to extract features of the partial iris image.

1.6.2 Requirement & Specifications

After a series of review on the state of art in iris image recognition system, the problem in the existing techniques on feature extraction was identified. The major problem is considering the entire iris for feature extraction and associating non iris element as features to represent an iris. Thus, with these findings from the literature review, the basic requirement is to identify the stable regions on the iris image for partial iris image recognition and hence, exploring a feature extraction method for partial iris image recognition was specified.

1.6.3 Designing Proposed Algorithms

Based on the requirement and specifications determined earlier derived from the findings of the literature review, the present research proposed a feature extraction method to identify the stable region of the iris for partial iris image recognition. Prior to extracting features of the partial iris image, the three different kinds of partial iris image models are designed and these are described in section 3.2. Each partial iris image model consists of two sub image regions on the iris and it is defined in the different location of the iris. Daugman's Rubber Sheet model (Daugman, 1994, 2004) has been used to unwrap partial iris image region into rectangular block of size. This design explains how to unwrap partial iris image region from

the different location of the iris and also analyzes the efficiency of unwrapping the partial iris image region for feature extraction process.

The Daubechies DB8 discrete wavelet transform has been employed to extract iris features for the three different kinds of partial iris image models. This design explains how to apply different wavelet filters to the unwrapped partial iris image and how a set of sub images are obtained at different resolution levels. This design also explains how to select features from the different levels of the wavelet transformed image and the reasons of using these features are also explained. From the extracted features it is also explained how to construct feature vector for the three different kinds of partial iris image models of each individual subject in the database. The feature encoding technique is also explained in this design to unique feature vector representation. Various criteria and evaluation methods are also identified in this stage.

1.6.4 Experiments and Analysis

The experiments are done to analyse the stability of features extracted from the three different kinds of partial iris image models. A series of experiments were carried out on CASIA Iris Image Database (CASIA-Iris Image Databases Version 1.0 (CASIA-IrisV1)) that includes 756 images from 108 different eyes or subjects. For each eye, 7 images are captured in two sessions, where three samples are collected in the first session and four in the second session. For each iris subjects, the three samples taken at the first session were chosen for training and all samples captured at the second session serves as test samples. The details on this sample database are described in section 4.2.

The intra-class and inter-class variability are measured based on fractional Hamming distance in order to select a suitable decision criterion for three different kinds of partial iris image models separately. Comparisons were performed between three kinds of partial iris image

models based on selected decision criterion. Through experiment the design suggested to use the features extracted from the inner right and inner left partial iris image model that produce better stability and discrimination. The EER (Equal Error Rate), FAR (False Accept Rate) and FRR (False Reject Rate) are calculated from the intra-class and inter-class comparisons of the inner right and inner left partial iris image models in order to evaluate the performance of the proposed method. The evaluation methods are described in detail in section 3.5.

1.7 Outline of the Dissertation

The outline gives brief introduction of each chapter in this dissertation.

Chapter 2 discusses on the various feature extraction methods that are used to extract features of the entire iris image, problems for the overall methodology of feature extraction methods and analysis of whether these methods are suitable to extract features of the partial iris image, discussions of issues like various similarity measurement techniques.

Chapter 3 discusses on partial iris image requirement analysis and proposed feature extraction method of the partial iris image recognition based on Daubechies DB8 discrete wavelet transform method. Various issues and factors are discussed throughout this chapter.

Chapter 4 discusses results and analysis to evaluate the performance of the proposed feature extraction method for partial iris image recognition. Information regarding sample sets used in the experiment, the performance of the use of the Partial iris image for recognition and the reasoning on the results obtained are explained in this chapter.

Chapter 5 discusses the findings, accomplishments, limitations and future enhancement of the research. The achievement shows the contribution of this research in partial iris recognition.

1.8 Summary

This chapter gives an introduction and general discussion for the research. The main goal of this research is to design and propose a feature extraction method of the partial iris image for partial iris recognition where capturing the entire iris may not be feasible. Research problems and scope are identified in this chapter. The following chapters will provide detailed discussions of this research. In short, this chapter aims to give the reader a better picture of the proposed partial iris image recognition method.

Chapter 2 Background & Survey

2.1 Introduction

This chapter starts with a review on the proposed architecture of a partial iris recognition system to understand its typical components. Based on the initial review in Chapter 1, the problem in existing techniques on feature extraction was identified. The major problem is considering the entire iris for feature extraction and associating non-iris element as features to represent an iris. Thus, this research proposed a feature extraction method to extract features of the partial iris image for partial iris image recognition. The partial iris image requirement for feature extraction is described in detail in Chapter 3.

The proposed solution identified the stable region of the iris for partial iris image recognition by extracting features with the proposed feature extraction method. Hence, this chapter reviews some of the notable feature extraction technique in the iris recognition era although these methods used the entire iris to extract unique features. This review on iris feature extraction aims to understand thoroughly the current feature extraction techniques, and analyze whether these methods can be used to extract features of the partial iris image.

2.2 Components of Partial Iris Recognition System

Figure 2.1 shows system architecture of the proposed partial iris recognition system which includes Pre-processing module, Partial iris generation module, Polar transformation of the generated partial iris module, Feature extraction module, Feature encoding module, Feature enrollment module and Feature verification module. However, this research is more focused on feature extraction of the partial iris image.

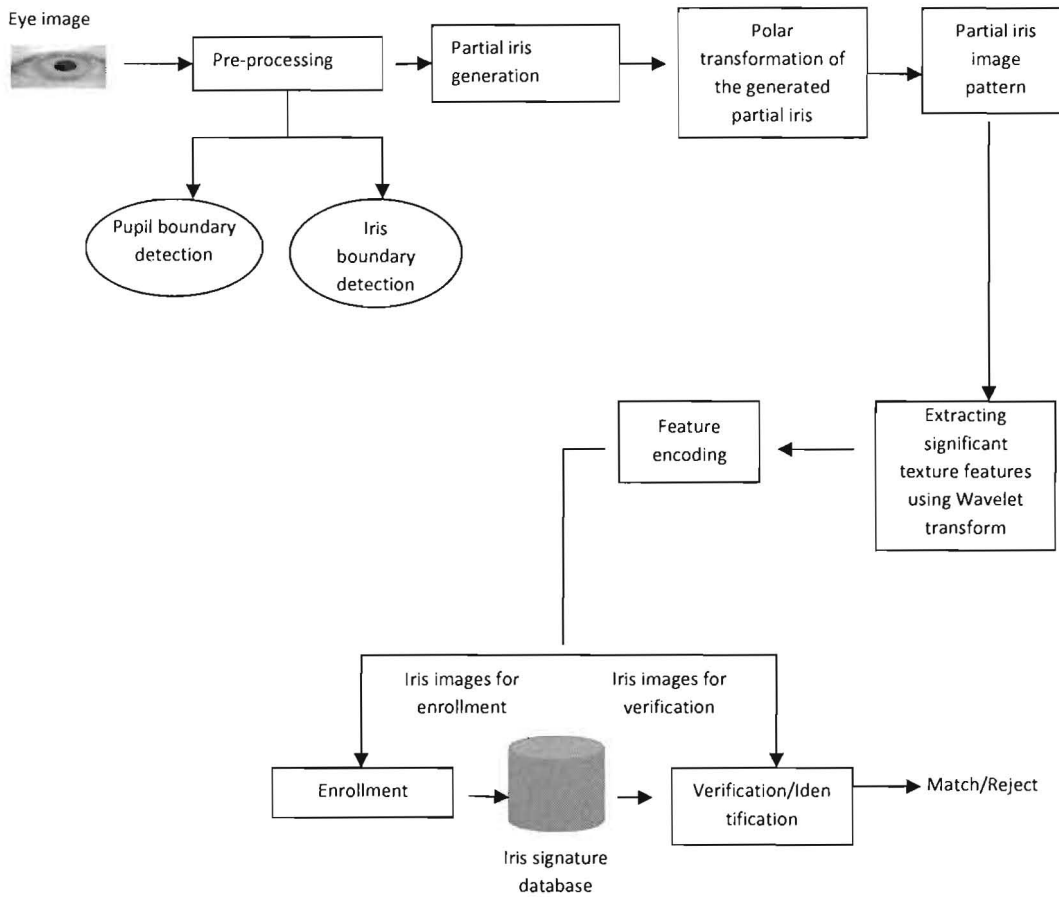


Figure 2.1 Components diagram of the proposed partial iris recognition system

The pre-processing module finds the pupil boundary and the iris boundary in the inputted raw iris image. The partial iris generation module design three different kinds of partial iris image models after studying and analyzing stability of the different region of the iris image and it is described in detail in Chapter 3. The polar transformation of the partial iris image module is used to unwrap partial iris image in to rectangular block of size from the different location of the iris in order to get the translation and scale invariant features. This is also described in detail in Chapter 3. The feature extraction module is the most crucial part of this research. In

this module, a feature extraction method based on Daubechies DB8 discrete wavelet transform is designed and proposed to extract discriminant texture features of the partial iris image. This designing and feature analysis are also described in detail in Chapter 3. The feature encoding module proposed a sign quantization technique for binary feature vector representation. The enrolment module extracts features of the partial iris image and stores them into database for later verification. In the partial iris image verification module, assuming that a test sample is from a specified subject, and the EER (Equal Error Rate), FAR (False Accept Rate) and FRR (False Reject Rate) are calculated from the intra-class and inter-class matching distance distributions in order to evaluate the performance of the proposed method. The evaluation method to evaluate the proposed feature extraction method is also described in detail in Chapter 3.

2.3 Feature Extraction Techniques

Feature extraction involves finding features to differentiate among iris images. The most important step in automatic iris recognition is the ability of extracting some unique attributes from the iris which help generate a specific code for each individual. Only the significant features of the iris must be encoded so that comparisons between templates can be made. Existing feature extraction processes are roughly divided into three major categories: the phase-based method such as Daugman (1993, 1994, 2001a, 2001b, 2003, 2004), zero-crossing representation by Boles & Boashash (1998) and texture analysis based method such as Wildes *et al.* (1996), Wildes (1997), Zhu *et al.* (2000), Ali & Hassanien (2003), Ma *et al.* (2003, 2004a, 2004b) and Kim *et al.* (2004). The well known phase based methods for feature processing are Gabor wavelet. The 1D wavelet is known for the Zero-crossing representation. The Laplacian of Gaussian filter and Gaussian-Hermite moments are used in texture analysis

based method. In this research, the texture analysis based method was also generated to extract features of the partial iris image.

Ophthalmologists Flom & Safir (1987) first noted the uniqueness of the iris patterns in 1987. Since then various algorithm have been proposed for iris image recognition. However, Iris image recognition is still an active area of research (Hollingsworth *et al.*, 2009) because of it's accuracy. Daugman (1993, 1994, 2001a, 2001b, 2003, 2004) used the 2D version of Gabor filters to extract the iris features and demodulates the output of the Gabor filters in order to compress the data. Demodulation is done by quantizing the phase information into four levels for each possible quadrant in the complex plane. These four levels are represented using two bits of data in the iris template. This process was repeated all across the iris with many wavelet sizes, frequencies, and orientations, to extract 2,048 bits. Wildes *et al.* (1996) and Wildes (1997) extract the iris texture features with a Laplacian of Gaussian filter constructed with four different resolution levels. Boles & Boashash (1998) proposed a technique to extract the features of the iris by fine-to-coarse approximations at different resolution levels based on the WT zero crossing representation and make use of 1D wavelets for encoding iris pattern data. Boles & Boashash (1998) calculated zero-crossing representation of 1D wavelet transform at various resolution levels of a virtual circle of an iris image to extract features of the iris. Vasta *et al.* (2005) used Log-Gabor filter for iris feature extraction. Ma *et al.* (2003) constructed a bank of spatial filters, whose kernels are suitable to extract local texture features of the iris. Ma *et al.* (2004a) use Gaussian-Hermite moments to characterize local variations of the intensity signals. Gaussian-Hermite moments are used for texture feature extraction with mathematical orthogonality and effectiveness for characterizing local details of the signal. The one-dimensional continuous wavelet transform is used to decompose iris image in Kim *et al.* (2004) where each decomposed one-

dimensional waveform is estimated by an optimal piecewise linear curve connecting a small set of node points, which is used as a feature vector and normalized correlation is used for matching the iris template. Hilbert Transform is used by Tisse *et al.* (2002) to create an analytic image, whose output is then encoded as an emergent frequency vector and an instantaneous phase in the feature extraction and encoding step. Some of the frequently used approaches for iris feature extraction are described below.

2.3.1 The Phase Based Method

Daugman (1993, 1994, 2001a, 2001b, 2003, 2004) uses convolution with 2-dimensional Gabor filters to extract the textural information from the iris images. A Gabor filter is constructed by modulating a sine/cosine wave with a Gaussian. This allows to provide the optimum conjoint localization both in space and frequency, but not localized in space. The decomposition of a signal is accomplished by using a quadrature pair of Gabor filters, with a real part specified by cosine modulated by a Gaussian, and an imaginary part specified by a sine modulated by Gaussian. The real and imaginary filters are also known as the even symmetric and odd symmetric components, respectively. The centre frequency is specified by the frequency of the sine/cosine wave, and the bandwidth of the filter is specified by the width of the Gaussian. A 2D Gabor filter over the image domain (x, y) is represented as

$$G(x, y) = e^{-\pi[(x-x_0)^2/\alpha^2 + (y-y_0)^2/\beta^2]} e^{-2\pi[u_0(x-x_0) + v_0(y-y_0)]} \quad (2.1)$$

where (x_0, y_0) specify position in the image, (α, β) specify effective width and length, and (u_0, v_0) specify modulation, which has spatial frequency $\omega_0 = \sqrt{\mu_0^2 + \nu_0^2}$.

The odd symmetric and even symmetric 2D Gabor filters are shown in Figure 2.2. Figure 2.2 illustrates the quadrature bandpass filters as image convolution kernels to extract iris structure at many scales of analysis. In Daugman (1994) system, the filters are multiplied by the raw image pixel data and integrated over their domain of support to generate coefficients which describe, extract, and encode image texture information.

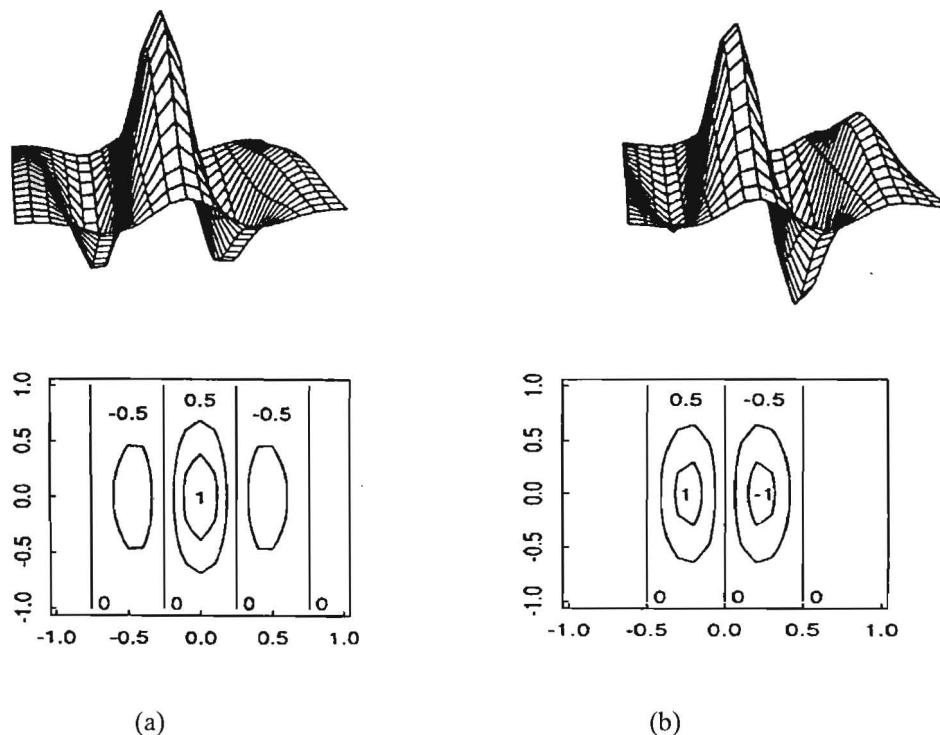


Figure 2.2 (a) and (b) even- symmetric and odd symmetric wavelet profiles together with their contour plots (adopted from Daugman (1994))

Daugman (1994) extracts the output of the Gabor filters in order to compress the data. This is done by quantizing the phase information into four levels, for each possible quadrant in the complex plane. These four levels are represented using two bits of data, so each pixel in the normalized iris pattern corresponds to two bits of data in the iris template. A total of 2048 bits

are calculated for the template. Daugman phase demodulation process is shown in Figure 2.3. This creates a compact 256-byte template, which allows for efficient storage and comparison of irises. The Daugman (1994) makes use of polar coordinates for normalization, therefore in polar form the filters are given as

$$(r, \theta) = e^{-i\omega(\theta-\theta_0)} e^{-(r-r_0)^2/\alpha^2} e^{-i(\theta-\theta_0)^2/\beta^2} \quad (2.2)$$

where (α, β) are the same as in Equation 2.1 and (r_0, θ_0) specify the centre frequency of the filter. The demodulation and phase quantization process can be represented as:

$$h_{\{\text{Re}, \text{Im}\}} = \text{sgn}_{\{\text{Re}, \text{Im}\}} \int_{\rho} \int_{\phi} I(\rho, \phi) e^{-i\omega(\theta_0-\phi)} e^{-(r_0-\rho)^2/\alpha^2} e^{-(\theta_0-\phi)^2/\beta^2} \rho d\rho d\phi \quad (2.3)$$

Where, $h_{\{\text{Re}, \text{Im}\}}$ can be regarded as a complex-valued bit whose real and imaginary parts are either 1 or 0 depending on the sign of the 2D integral. $I(\rho, \theta)$ is the raw iris image in a dimensionless polar coordinate system that is size and translation invariant. (α, β) are the multi-scale 2D wavelet size parameters, spanning an 8-fold range from 0.15mm to 1.2mm on the iris; ω is wavelet frequency, spanning 3 octaves in inverse proportion to β . (r_0, θ_0) represent the polar coordinates of each region of iris for which the phasor coordinates $h_{\{\text{Re}, \text{Im}\}}$ are computed. Equation 2.3 determines each of the 2048 bits in an iris code, across multiple scale of analysis (set by parameters α and β) and across all of the sampled position (set by polar coordinate parameter r and θ) within the defined zones of analysis of the iris image.

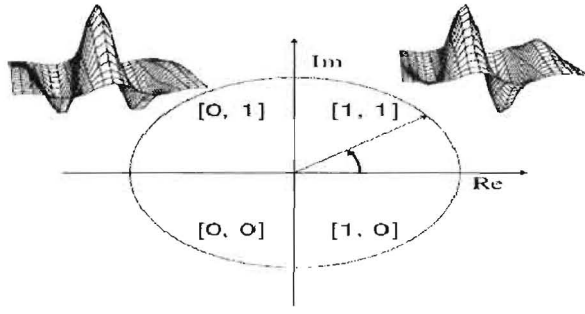


Figure 2.3 Daugman phase demodulation process (adopted from Daugman (2004))

However, one weakness of the Gabor filter in which the even symmetric filter will have a DC component whenever the bandwidth is larger than one octave (Field, 1987) that means DC component may affect of the computed iris code by the strength of illumination due to DC response in real parts of the filtered image. Another problem of the characteristics vectors generated by this method requires 256 or more dimensions or at least 256 bytes, where one byte assigned to one dimension. Thus, there is a problem in that practicability and efficiency are counteracted when the Gabor filters is used in the field if low capacity information is required.

Daugman (1994) phase based method extract phase information by spanning 8-fold range from the entire iris across all of the sampled position set by polar coordinate parameter r and θ in order to encode 2048 bit iris code. In the proposed approach, a partial iris image or a significant portion of the iris is utilized to extract features. Thus, it is needed to make use of whole component of the partial iris image to extract unique features. The only phase information extracted from the sampled position set by polar coordinate parameter r and θ of the partial iris image is not suitable to extract unique features.

2.3.2 Zero-Crossing Representation Based Method

Boles & Boashash (1998) proposed a technique to extract and represent the features of the iris by fine-to-coarse approximations at different resolution levels based on the WT zero crossing representation. The mother wavelet is defined as the second derivative of a smoothing function $\theta(x)$.

$$\psi(x) = \frac{d^2\theta(x)}{dx^2} \quad (2.4)$$

The zero crossings of dyadic scales of these filters are then used to encode features.

The wavelet transform of a signal $f(x)$ at scale s and position x are given by:

$$\begin{aligned} W_s f(x) &= f * \left(s^2 \frac{d^2\theta(x)}{dx^2} \right) (x) \\ &= s^2 \frac{d^2}{dx^2} (f * \theta_s)(x) \end{aligned} \quad (2.5)$$

where $\theta_s = (1/s)\theta(x/s)$. $W_s f(x)$ is proportional to the second derivative of $f(x)$ smoothed by $\theta_s(x)$, and the zero crossings of the transform correspond to points of inflection in $f * \theta_s(x)$.

The motivation for this technique is that zero-crossings at the different resolution level of the dyadic wavelet transformed image correspond to significant features. Figure 2.4 illustrates the zero-crossing representation of the iris.

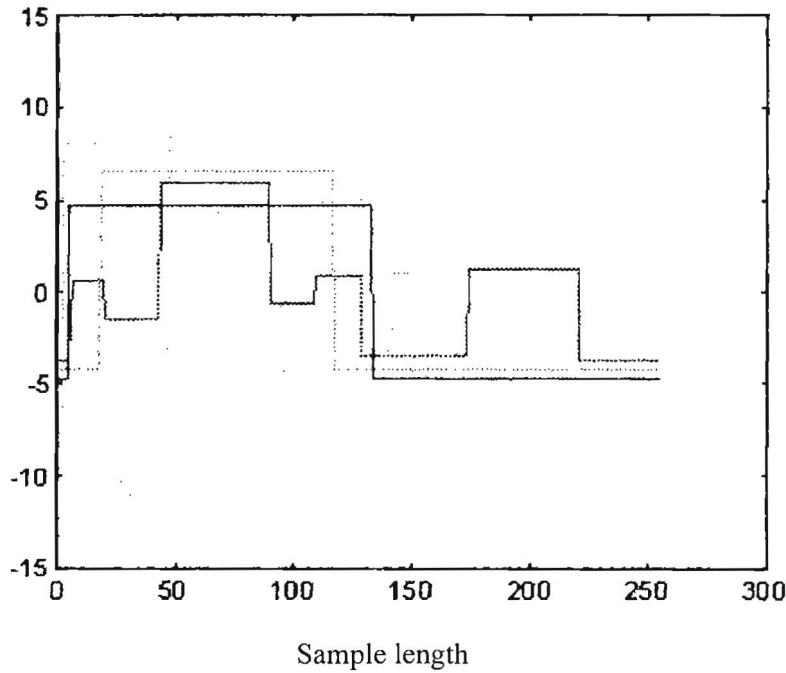


Figure 2.4 Zero-crossing of WT (adopted from Boles & Boashash (1998))

Boles & Boashash (1998) decomposed one dimensional signals computed on circles in the iris and used zero-crossing of the decomposed signals for the feature representation. The problem of this method is that the number of zero-crossing can differ among iris image samples of an identical iris due to noises (Kim *et al.*, 2006). The size of partial iris image is smaller than complete iris image. Thus, number of zero crossing will be decreased predominantly if this technique applied to partial iris image. The lowest number of zero-crossing information may not be enough to produce discriminant features for partial iris image recognition.

2.3.3 Texture Analysis Based Method

The distinctive spatial characteristics of the iris are apparent at variety of scales. The distinguishing structures ranges from the overall shape of the iris to the distribution of tiny crypts and detailed texture (Wildes *et al.*, 1996). To capture this range of spatial structures,

the iris image is represented in terms of two-dimensional bandpass decomposition. Wildes *et al.* (1996) and Wildes (1997) used Laplacian of Gaussian filters to extract the distinctive spatial characteristics of the iris. The filters are mathematically defined as:

$$\nabla G = -\frac{1}{\pi\sigma^4} \left(1 - \frac{\rho^2}{2\sigma^2} \right) e^{-\rho^2/2\sigma^2} \quad (2.6)$$

where σ is the standard deviation of the Gaussian and ρ is the radial distance of a point from the centre of the filter. A Laplacian pyramid is constructed with four different resolution levels which are shown in Figure 2.5 in order to generate a compact iris image data. In order to extract discriminating attributes from the different iris images Wildes *et al.* (1996) used an area based, image registration technique. This technique seeks mapping function $(u(x, y), v(x, y))$ such that for all (x, y) , the pixel value at $(x, y) - (u(x, y), v(x, y))$ in the data image is close to that at (x, y) in the model image. In this technique, (x, y) are taken over the whole iris regions.

With the model and data images accurately and precisely registered, an appropriate match metric is used in Wildes *et al.* (1996) based on integrating pixel differences over spatial position within each frequency band of the image depicted in Figure 2.5. Spatial correlation captures this notion. The correlations are performed over small block of pixels (8×8) in each spatial frequency band. The goodness of match is derived for each band by combining the block correlation values via the median statistic. The four goodness of match value that has been computed needed to be combined in order to make a final decision. The final decision is obtained from a Fisher linear discriminant based on the strength of match of each frequency band.

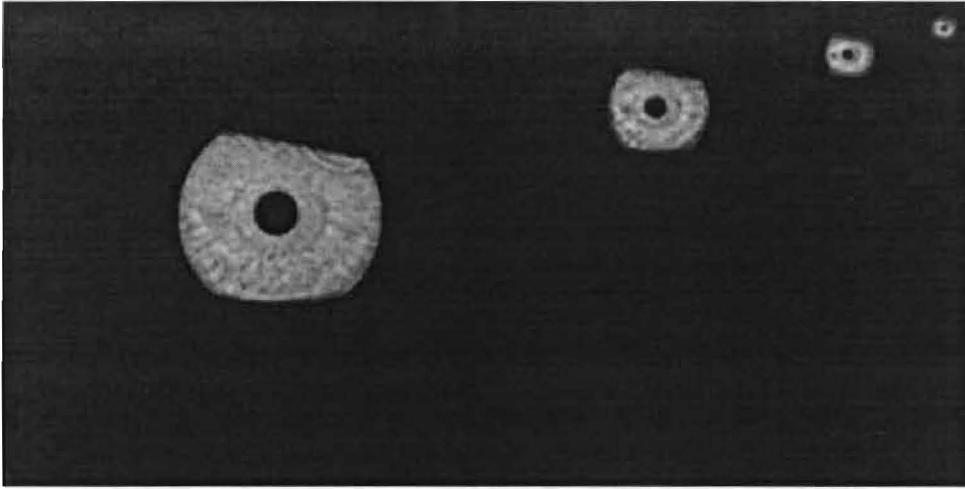


Figure 2.5 Multiscale representation for iris pattern (adopted from Wildes *et al.* (1996))

The Wildes *et al.* (1996) approach made use of more of the available data, by not binarizing the bandpass filtered result, and hence might be capable of finer distinctions; however, it yields a less compact representation and this approach uses a very computational image registration technique (Ma *et al.*, 2004b; Chen *et al.*, 2009).

Ma *et al.* (2003) constructed a bank of spatial filters, whose kernels are suitable to extract local texture features of the iris. A bank of filters is constructed to dependably gain frequency information in the spatial domain where one can extract information of an image at a certain orientation and scale using some filtering technique, since coefficient of the filtered image effectively points the frequency distribution of an image. The difference between Gabor filter and defined Spatial filter lies in the modulating sinusoidal function where Gabor filter is modulated by an oriented sinusoidal function, whereas the Spatial filters is modulated by a circularly symmetric sinusoidal function which is as follows:

$$G(x, y, f) = \frac{1}{2\pi\delta_x\delta_y} \exp\left[-\frac{1}{2}\left(\frac{x^2}{\delta_x^2} + \frac{y^2}{\delta_y^2}\right)\right] M_i(x, y, f), i = 1, 2.$$

$$M_1(x, y, f) = \cos\left[2\pi f(\sqrt{x^2 + y^2})\right], \quad (2.7)$$

$$M_2(x, y, f) = \cos\left[2\pi f(x \cos \theta + y \sin \theta)\right],$$

where, $M_i(x, y, f)$ denotes the modulating function, M_1 and M_2 are the modulating function of the spatial filter and Gabor filter, f is the frequency of the sinusoidal function, δ_x and δ_y are the space constants of the Gaussian envelope along the x and y axis and θ denotes the orientation of the Gabor filter. When δ_x equals to δ_y one can obtain a bandpass filter with a specific center frequency. When δ_x equals to δ_y are different, it not only considers information from every orientation but also demoeed more interest in information in x or y direction, defined by δ_x and δ_y . This demoed difference from Gabor filter which can only provide information of an image at certain information. The differences between Gabor filter and spatial filters are depicted in Figure 2.6. Ma *et al.* (2003) mentioned useful iris information distributes in a specific frequency range. They used the defined spatial filters in two channels to acquire the most discriminating features. The input parameter for δ_x and δ_y used in the first channel are 3 and 1.5, and the second channel 4.5 and 1.5. They used multiple filters with different frequency response for the entire iris image to extract discriminating features since different irises have distinct dominant frequencies. According to this scheme, filtering the entire iris image (48×512) with multichannel spatial filters results in:

$$F_i(x, y) = \iint I(x_1, y_1) G_i(x - x_1, y - y_1) dx_1 dy_1; \quad i = 1, 2 \quad (2.8)$$

where G_i is the i the channel of the spatial filters, $I(x, y)$ denotes the iris image, and $F_i(x, y)$ is the filtered image. They extract statistical features in each 8×8 small block to characterize local texture information of the iris. The total number of small block is $[(48 \times 512) / (8 \times 8) \times 2] = 768$. For each small block, two feature values are captured. This generates 1536 feature components. The feature values used in the algorithm are the mean m and the average absolute deviation σ of the magnitude of each filtered block defined as

$$m = \frac{1}{n} \sum_w |F_i(x, y)|, \quad \sigma = \frac{1}{n} \sum_w ||F_i(x, y)| - m|, \quad (2.9)$$

where, $F_i(x, y)$ is the filtered image, w is an 8×8 block in the filtered image, n is the number of pixels in the block w , and m is the mean of the block w .

Ma *et al.* (2003) feature extraction technique may extract useful feature components from the entire iris image. They divided filtered normalized iris image into 8×8 small blocks to extract statistical features. They calculated mean and average absolute deviation value of those blocks and stored as features. By this way, they extract 1536 feature components from the normalized iris image. But, this feature extraction technique may not be suitable to extract features of the partial iris image. Since, the size of the normalized partial iris image is predominantly reduced as compared to the normalized entire iris image.

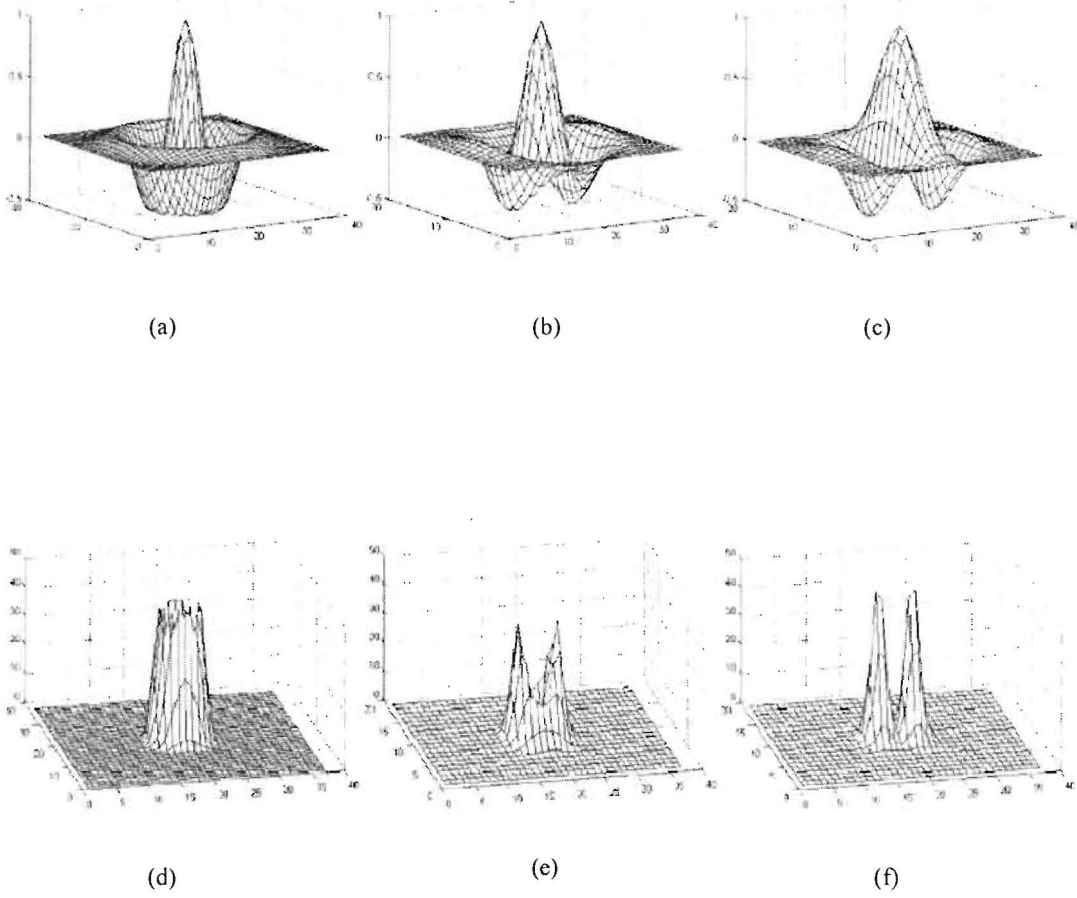


Figure 2.6 (a) Spatial filter with $\delta_x = \delta_y$ (b) spatial filter with $\delta_x > \delta_y$ (c) Gabor filter (d), (e), and (f) are the Fourier spectra of (a), (b), and (c) (image taken from Ma *et al.* (2003))

After filtering the normalized partial iris image only significant information remains. Thus, it is required to consider the remaining significant information as features of the partial iris image in order to produce discriminant features among the iris images. If the normalized filtered partial iris image is divided into 8×8 small blocks and consider only mean and average absolute deviation as features, only few feature components should remain. These feature components may not produce discriminant features among the partial iris images.

Lim *et al.* (2001) employed Haar wavelet transform to extract features from the iris image region. They applied Haar wavelet transform four times to the normalized iris image. From multi-dimensionally filtering, a feature vector with 87 dimensions is computed. They extract 84 features corresponding to high pass filter of the 4th level of wavelet transformed image and each average value for the three remaining high pass filter areas. This generates a total of 87 feature components. The dimension of the resulting feature vector is 87. Figure 2.7 illustrates Haar wavelet as a basis function.

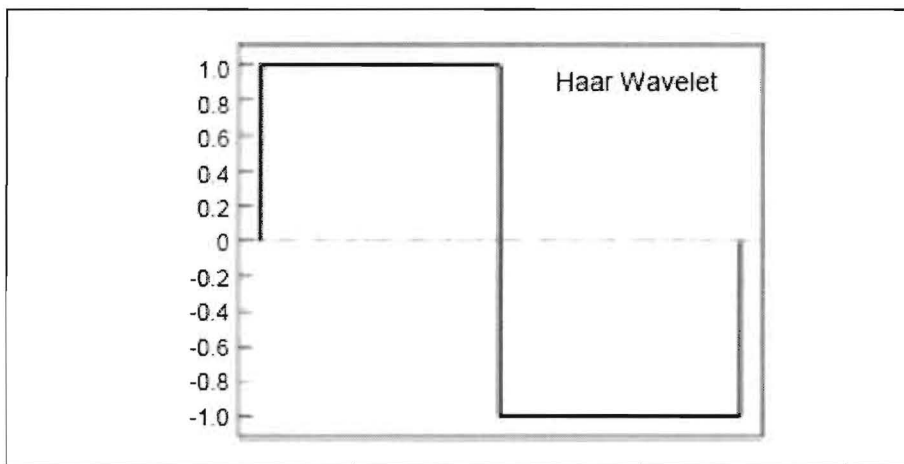


Figure 2.7 Haar mother wavelet (image taken from Lim *et al.* (2001))

Lim *et al.* (2001) compare the use of Gabor transform and Haar wavelet transform, and show that the recognition rate of Haar wavelet transform is slightly better than Gabor transform by 0.9%. However, Haar wavelet functions have disadvantages that the characteristic values are discontinuous and rapidly changing and that high resolution of the images cannot be obtained in a case where the images are again decompressed after they have been compressed (Wang *et al.*, 1998).

Poursaberi & Araabi (2007) proposed an iris recognition method for partially occluded images. In their works, they have emphasized on iris segmentation to cope with occlusion that occurs due to eyelids and eyelashes. The two different segmentations of iris were presented in their works. In the first algorithm, a circle is located around the pupil with an appropriate diameter. The iris area encircled by the circular boundary is used for recognition purposes. In the second method, again a circle is located around the pupil with a large diameter. However, this time only the lower part of the encircled iris area is utilized for recognition. Wavelet based texture features were used for recognition.

In their first method, the collarette boundary of the irises was localized by choosing a certain radius from the edge of pupil and the entire collarette region of the iris was used for feature extraction. In their second method, the iris boundary of the eye images was localized by choosing an iris radius of 38 pixels from the edge of the pupil which includes collarette region and some part of the ciliary region. The lower part of this localized iris region was used for feature extraction. However, it is observed that the upper and lower parts of the localized collarette region of the iris are also occluded by the eyelids and eyelashes and the experiment results that are described in chapter 4 clarify that these are very important causes for false result during recognition.

Poursaberi & Araabi (2007) utilized Daubechies 2 wavelet transform to extract features from iris images. The Daubechies 2 wavelet transform was applied four times in their first method and three times in their second method. They composed of feature vectors with 408 binary matrix by combining features in the vertical and horizontal approximation coefficients of level-4 wavelet transformed image in their first method. They comprised of feature vectors with 544 binary matrix by combining features in the vertical and horizontal approximation coefficients of level-3 wavelet transformed image in their second method. Although,

Poursaberi & Araabi (2007) reported that they have achieved promising performance (99.31% correct recognition rate) through their second method, they still cannot cope with the occlusion problem in a situation while collarette regions are occluded by the eyelids and eyelashes. Figure 2.8 shows some of the iris images in which collarette area is occluded by eyelids and eyelashes that are not recognized as correct according to methods proposed by Poursaberi & Araabi (2007).

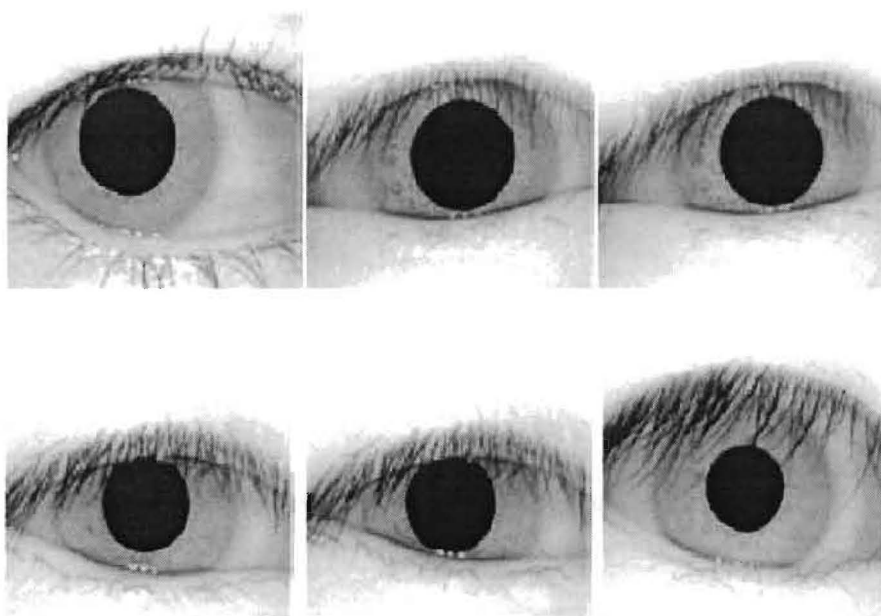


Figure 2.8 Collarette area is occluded by eyelids and eyelashes which are not recognized as correct by the proposed methods of Poursaberi & Araabi (2007).

However, another disadvantage of this method is using Daubechies 2 wavelets as the basis functions for the decomposition. Daubechies wavelets are classified according to the number of vanishing moments, N . The smoothness of the wavelets increases with the number of vanishing moments. For the case when $N=1$, the Daubechies scaling and wavelet function resembles that of the Haar wavelet transform and are discontinuous. It is desirable to have smooth wavelets and therefore N is increased. Daubechies wavelet transform with longer

length filters has better frequency properties (Daubechies, 1988). Although the Daubechies 2 wavelet is continuous, its derivative is discontinuous. For N greater than 2, the wavelet and its derivative are both continuous. It has been shown in applications such as compression, noise removal and singularity detection, that the number of vanishing moments plays a key role for efficient coding of signals (Mallat, 1998).

2.3.4 Other Algorithms

Ma *et al.* (2004b) proposed a feature extraction technique based on randomly distributed blocks in the iris region by characterizing local sharp variations of the iris. They construct a set of one-dimensional intensity signals from the two dimensional normalized iris images. They employed a special class of wavelet to represent the resulting 1-D intensity signals. Then, the position sequence of local sharp variations points in such signals are recorded as features.

Ma *et al.* (2004a) makes an attempt to reflect shape information of the iris by analyzing local intensity variations of an iris image. The shape such as freckles, coronas, stripes and furrows etc. can be considered as an elementary component of the iris texture. These different components of the iris texture can cause significant local variations in the intensity signals. The shape of an iris block determines both the number of the intensity signals which this block can affect and the interval of significant local variations. Then, a set of one-dimensional (1D) intensity signals is constructed to contain the most important local variations of the original 2D iris image. Gaussian–Hermite moments of such intensity signals reflect to a large extent their various spatial shapes and are used as distinguishing features.

1D Log-Gabor filter wavelet technique was employed in Roy & Bhattacharya (2008) in order to extract deterministic feature sequence of the iris images and the extracted feature sequence

is used to train the support vector machine (SVM). The multi-objectives genetic algorithm (MOGA) was applied to optimize the features sequence and to increase the overall performance based on the matching accuracy of the SVM. Cumulative sum based grey change analysis method was adopted in Ko *et al.* (2007) in order to extract iris feature.

The kind of filters used by the existing approaches for feature extraction, the kind of features and drawbacks of these technique and features for iris image recognition are summarized in Table I.

Table I The comparison among the existing methods

Methods	Filters	Kind of feature	Drawbacks
Daugman (1993, 1994, 2001a, 2001b, 2003, 2004)	2-D Gabor	Binary feature vector (extracted phase information and encoded it into 2048 bit iris code)	<ul style="list-style-type: none"> • The weakness of Gabor filter in which the even symmetric filter will have a DC component whenever bandwidth is larger than one octave (Field, 1987) i.e. the extracted features using this method are affected by the strength of illumination. • Another problem of the characteristics vectors generated by this method requires 256 or more dimensions or at least 256 bytes, where one byte assigned to one dimension. There is a problem in that practicability and efficiency are counteracted when the Gabor filters is used in the field if low capacity information is required.
Wildes <i>et al.</i> (1996) and Wildes (1997)	Laplacian of Gaussian	Image (Laplacian pyramid to represent the spatial characteristics of iris image)	<ul style="list-style-type: none"> • The Wildes approach made use of more of the available data, by not binarizing the bandpass filtered result; however, it yields a less compact representation and this approach uses a computational image registration technique (Ma <i>et al.</i>, 2004b; Chen <i>et al.</i>, 2009). • This technique of representing features needs a time consuming matching process. It may be suitable for identification phase and not for recognition (Roy & Bhattacharya, 2008)

Ma <i>et al.</i> (2004b)	Special Wavelet	1D integer- valued feature vector	<ul style="list-style-type: none"> This technique constructs a set of one dimensional intensity signals from the two dimensional normalized iris images. A special class of wavelet is used to represent the 1-D intensity signals. The position sequence of local sharp variations points in such signals selected as unique features. The problem of this method is relatively slow feature extraction method and cannot cope with occlusions problem (Roy & Bhattacharya, 2008).
Lim <i>et al.</i> (2001)	Haar Wavelet	Binary feature vector	<ul style="list-style-type: none"> This method used Haar wavelet transform to extract unique features. However, Haar wavelet functions have disadvantages that the characteristics values are discontinuous and rapidly changes and that high resolution of the images cannot be obtained in a case where the images are again decompressed after they have been compressed (Wang <i>et al.</i>, 1998). The features obtained by this method give poor recognition rate, big EER, and cannot cope with occlusions problem (Roy & Bhattacharya, 2008).
Boles & Boashash, (1998)	Dyadic wavelet	1D signature	<ul style="list-style-type: none"> This method decomposed one dimensional signals computed on circles in the iris and used zero-crossing of the decomposed signals as unique features. The problem of this method is that the number of zero-crossing can differ among iris image samples of an identical iris due to noises (Kim <i>et al.</i>, 2006). The features obtained by this method give low recognition rate, high EER (Roy & Bhattacharya, 2008).
Poursaber i & Araabi (2007)	Daubechies 2	Binary matrix	<ul style="list-style-type: none"> The features obtained by this method produce incorrect recognition result while collarette boundary of the irises is occluded. Daubechies wavelet transform with longer length filters has better frequency properties (Daubechies, 1988). However, this method used Daubechies 2 wavelet transform for feature extraction.

2.4 Similarity Measurement Techniques

The goal of similarity measurement techniques in iris recognition is to match the iris feature and determine whether the feature comes from an authentic one or an imposter or simply to get the similarity and dissimilarity value among the iris images in the database. The different similarity measurement techniques used in iris recognition are explained below.

2.4.1 Hamming Distance

Daugman (2004) first utilize the Hamming distance technique to measure the similarities among the iris templates. The Hamming distance gives a measure of how many bits are the same between two bit patterns. A decision can be made as to whether the two patterns were generated from the different or the same iris images by calculating the Hamming distance of two bit patterns.

In comparing the bit patterns F_A and F_B , the Hamming distance, HD, is defined as sum of disagreeing bits (sum of the exclusive –OR between F_A and F_B) over N , the total number of bits in the bit pattern.

$$HD = \frac{1}{N} \sum_{j=1}^N F_A(j) \text{ XOR } F_B(j) \quad (2.10)$$

Since an individual iris region contains features with high degrees of freedom, each iris region will produce a bit-pattern which is independent to that produced by another iris, on the other hand, two iris codes produced from the same iris will be highly correlated (Masek, 2003a).

If two bit patterns are completely independent, such as iris templates generated from different irises, the Hamming distance between the two patterns should equal 0.5 (Daugman, 1993).

This occurs because independence implies the two bit patterns will be totally random, so there is 0.5 chance of setting any bit to 1, and vice versa. Therefore, half of the bits will agree and half will disagree between the two patterns. If two patterns are derived from the same iris, the Hamming distance between them will be close to 0.0, since they are highly correlated and the bits should agree between the two iris codes (Masek, 2003a).

2.4.2 Normalized Correlation

Wildes *et al.* (1996) make use of normalized correlation between the acquired and database representation for goodness of match. This is represented as:

$$\frac{\sum_{i=1}^n \sum_{j=1}^m (p_1[i, j] - \mu_1)(p_2[i, j] - \mu_2)}{nm\sigma_1\sigma_2} \quad (2.11)$$

where p_1 and p_2 are two images of size $n \times m$, μ_1 and σ_1 are the mean and standard deviation of p_1 , and μ_2 and σ_2 are the mean and standard deviation of p_2 .

Normalized correlation is advantageous over standard correlation, since it is able to account for local variations in image intensity that corrupt the standard correlation calculation (Masek, 2003a).

2.4.3 Weighted Euclidean Distance

The Weighted Euclidean Distance (WED) is employed by Zhu *et al.* (2000) to measure similarity among the iris templates. The Weighted Euclidean Distance (WED) can be used to compare two templates, especially if the template is composed of integer values. The

weighting Euclidean distance gives a measure of how similar a collection of values are between two templates. This is represented as:

$$WED(k) = \sum_{i=1}^N \frac{(f_i - f_i^{(k)})^2}{(\delta_i^{(k)})^2} \quad (2.12)$$

where f_i is the i^{th} feature of the unknown iris, and $f_i^{(k)}$ is the i^{th} feature of iris template, k , and $\delta_i^{(k)}$ is the standard deviation of the i^{th} feature in iris template k . The unknown iris template is found to match iris template k , when WED is a minimum at k .

2.4.4 Nearest Center Classifier

Ma *et al.* (2003) employed the nearest center classifier method for classification in a low dimensional feature space. This is represented as:

$$m = \arg \min_{1 \leq i \leq c} d_n(f, f_i); \quad n = 1, 2, 3.$$

$$d_1(f, f_i) = \sum_j |f^j - f_i^j|$$

$$d_2(f, f_i) = \sum_j (f^j - f_i^j)^2 \quad (2.13)$$

$$d_3(f, f_i) = 1 - \frac{f^T f_i}{\|f\| \|f_i\|}$$

where f and f_i are the feature vector of an unknown sample and the i^{th} class, respectively, f^j and f_i^j are the j^{th} component of the feature vector of the unknown sample and that of the

i^{th} class, respectively, c is the total number of classes, $\| \cdot \|$ indicates the Euclidean norm, $d_n(f, f_i)$ denotes similarity measure, d_1, d_2 and d_3 are L_1 distance measure, L_2 distance measure (Euclidean distance) and cosine similarity measure, respectively. The feature vector f is classified into the m^{th} class, the closest mean, using similarity measure $d_n(f, f_i)$.

2.5 Summary

This chapter gives a review on various feature extraction techniques of iris recognition, the phase based method, Zero-crossing representation and texture analysis based method. These feature extraction techniques have been analyzed whether these techniques can be generated to extract features of the partial iris image. The analysis has been accomplished based on two criteria to ascertain whether the existing approaches can be used to extract features of the partial iris image. They are based on the kind of filters used to extract iris features, the kind of features used in the existing approaches for iris recognition. Several problems have been mentioned during analysis of these feature extraction techniques, the kind of feature used for recognition in context of use to extract features of the partial iris image. From the comparison table it is also ascertain that most of the existing feature extraction method cannot cope with occlusion problem. Hence, a partial iris image recognition method needs to be explored in order to extract features of the partial iris image that can overcome the occlusion problems in the existing approaches. The designing of different kinds of partial iris image models and analysis of the proposed feature extraction method of the partial iris image is described in Chapter 3. The different similarity measurement techniques used in iris recognition are also discussed in this Chapter.

Chapter 3 Partial Iris Image Requirement & Feature Extraction for Partial Iris Recognition

3.1 Introduction

Following the previous chapters, it is clear that the existing approaches produce false result due to partially occluded iris images. The existing feature extraction techniques used to extract iris features from the entire iris and keep the data into a database during enrollment for further verification. But, it is observed that unfortunately 1/3 of the entire iris is obstructed due to partially occluded by the eyelids and some part of the iris is often covered by eyelashes (Wei *et al.*, 2005), improper eye opening and by other extraneous artefacts in most of the cases. This deformations cause abundant loss of characteristics of information and associating non-iris element as features to represent an iris in the existing feature extraction process. In order to overcome these problems, this research designed and developed a feature extraction technique for partial iris image recognition in order to identify/verify a person by their significant portion of the iris. Therefore, the existing feature extraction techniques have been studied and analyzed in chapter 2 in order to investigate whether these techniques can be used to extract features of the partial iris image. However, from the previous chapter on background survey, it is clear that the existing feature extraction techniques do not fit to extract features of the partial iris images. Several problems have been mentioned in the previous chapter during analysis of these feature extraction techniques for extracting features of the partial iris images.

This chapter starts with an analysis of the partial iris image requirement prior to the explanation of feature extraction method of the partial iris image for partial iris recognition.

These analyses of partial iris image requirement discussed about the stable region of the iris that could be used to extract features of the partial iris image for partial iris recognition. Based on analysis and observation in the CASIA iris image database, the three different kinds of partial iris image models are designed. Each partial iris image model consists of two sub image regions on the iris and it is defined in the different location of the iris. Daugman's Rubber Sheet Model (Daugman, 1994, 2004) has been used to unwrap partial iris image in to a rectangular block of size. This design explains how to select different partial iris image region on the iris image could be selected. The designing of Rubber Sheet Model also explains how to unwrap partial iris image region from the different location of the iris and also analyzes the efficiency of unwrapping of the partial iris image region for feature extraction process.

The Daubechies DB8 discrete wavelet transform has been generated to extract iris features for the three different kinds of partial iris image models. This design explains how to apply different wavelet filters to the unwrapped partial iris image and how a set of sub images are obtained at different resolution levels. This design also explains on how to select features from the different levels of the wavelet transformed image and the reasons of using these features are also explained. From the extracted features it is also explained how to construct feature vector for the three different kinds of partial iris image models of each individual subject in the database. The feature encoding technique is also explained in this design to unique feature vector representation.

The Hamming distance similarity measurement technique (Daugman, 2004) is employed in order to classify among the extracted templates for the three different kinds of partial iris image models in the database. Lastly, several evaluation methods have been illustrated in

order to assess the performance of the feature extraction method for partial iris image recognition.

3.2 Partial Iris Image Requirement

In this research, it is discovered that the most useful discriminating and individually unique iris patterns are presented in the iris region near to the pupil boundary which contains the collarette that appears as a zigzag pattern (Ma *et al.*, 2003, 2004b; He & Shi, 2005; Hollingsworth *et al.*, 2008; Roy & Bhattacharya, 2008). The collarette region is the most important part of the iris complex patterns since it is usually less sensitive to the pupil dilation and less affected by the eyelid and eyelashes (He & Shi, 2005; Roy & Bhattacharya, 2008). From the empirical study, it is found that collarette region of the iris is generally concentric with the pupil, and radius of this area is restricted in a certain range (He & Shi, 2005). The collarette region of the iris is isolated by selecting a radius of pixels randomly from the edge of the pupil and the selected region usually contains the collarette region as well. Figure 3.1 shows the collarette boundary of the iris. However, it is observed that the upper and lower parts of the localized collarette iris region are partially covered by the eyelids and eyelashes in most of the cases which are very important sources to create false result during recognition. In order to avoid these difficulties, this research designed different partial iris image models and proposed a Daubechies DB8 discrete wavelet based feature extraction method that relaxes the requirement of using a major part of the iris image, which can enable partial iris image recognition.

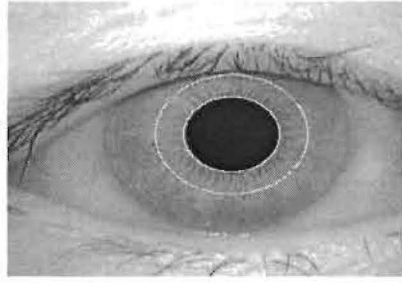


Figure 3.1 Collarette boundary of the iris

The significant part of the iris image is selected from the collarette region of the iris to extract unique features. The three different kinds of partial iris image models are analysed in order to justify the stability of the extracted features from the significant part of the collarette region of the iris. Figure 3.2 illustrates the eight sub divided regions of the iris image. The sub divided iris regions $I_1 - I_4$ belongs to the collarette boundary of the iris and regions $I_5 - I_8$ relies near to the sclera boundary of the iris according to the proposed sub divided iris structure.

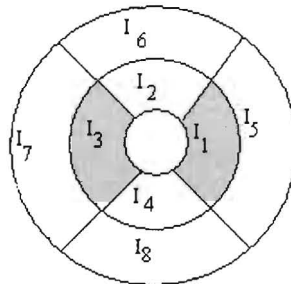


Figure 3.2 Proposed partial iris model

- a. **Inner right and inner left model:** In this model, the partial iris image from the region I_1 and I_3 were selected as shown in Figure 3.2. The unique texture characteristics information was extracted from the inner right and inner left sub

image (I_1 and I_3) separately. The extracted characteristics information of the inner right and inner left sub images are concatenated to make a unique characteristics vector.

- b. **Outer right and outer left model:** In this model, the partial iris image was selected from the region I_5 and I_7 as shown in Figure 3.2. The unique characteristics information was extracted from the outer right and outer left sub image (I_5 and I_7) separately. The extracted characteristics information of the outer right and outer left sub images are concatenated to make a unique characteristics vector.
- c. **Upper and lower model:** In this model, the partial iris image from the region I_2 and I_4 were selected as shown in Figure 3.2. The unique characteristics information was extracted from the upper and lower sub image (I_2 and I_4) separately. The extracted characteristics information of the upper and lower sub images are concatenated to make a unique characteristics vector.

The empirical experiment has been performed on 756 iris images from 108 different subjects (or classes) for the three different kinds of partial iris models in the CASIA iris image database. From the empirical experiment performed on three different kinds of partial iris image models, the partial iris image from the region I_1 and I_3 namely inner right and inner left sub image model is selected to extract unique features that can enable partial iris image recognition system. The extracted characteristics information from the inner right and inner left sub images are concatenated to make a unique characteristics vector. The characteristics vector is encoded for unique feature vector representation. This unique feature vector ultimately is used for partial iris image recognition. The brief analyses are given below to select behind inner right and inner left sub image model (I_1 and I_3).

It is discovered that the most useful discriminating and individually unique iris patterns are present in the iris region near to the pupil boundary which contains the collarette that appears as a zigzag pattern (Ma *et al.*, 2003, 2004b; He & Shi, 2005; Roy & Bhattacharya, 2008). The iris image closer to the pupil is more useful than the one closer to the sclera (Bowyer *et al.*, 2008). The inner right and inner left sub image model (I_1 and I_3) and the upper and lower sub image model (I_2 and I_4) lie in the collarette boundary of the iris. The upper and lower sub image model (I_2 and I_4) belonging to upper and lower parts of the collarette region of the iris. However, it is observed that the upper and lower parts of the collarette iris region are partially covered by the eyelids and eyelashes in maximum cases which are very important sources that contribute to false result during recognition. From these observations, the collarette iris region (I_1 and I_3) namely inner right and inner left sub image models were selected so that feature extraction is only performed in the regions of no occlusion.

The stability of iris features extracted from the upper and lower sub image model (I_2 and I_4) is evaluated in this research. The efficiency of upper and lower sub image model (I_2 and I_4) is evaluated by extracting features through using the proposed partial iris image feature extraction algorithm described in section 3.3. The stability of the extracted iris features is measured by performing intra-class and inter-class comparison among the templates extracted from the upper and lower sub image model in the iris image database. It is observed that the decision cannot be made without uncertainty with the templates extracted from the upper and lower sub image model (I_2 and I_4) in the database. From the acquired results described in section 4.3, it was observed that the stability of the extracted features from the upper and lower sub image model (I_2 and I_4) is greatly affected by the noise occluded by the eyelids and eyelashes.

The outer right and outer left sub image model (I_5 and I_7) lies down far away from the pupil boundary. Ma *et al.* (2004b) found that the iris regions closer to the sclera contains few texture characteristics and are easily occluded by eyelids and eyelashes. From the experiment with the outer right and outer left sub image model (I_5 and I_7) described in section 4.3, it is also observed that outer right and outer left sub image model contains few texture characteristics and extracted features may alter due to occlusion. The outer right and outer left sub image model (I_5 and I_7) may also be corrupted by the incorrect outer boundary detection between the iris and sclera especially when there is a little contrast between iris and sclera regions (He & Shi, 2005).

The better stability of the extracted features from the inner right and inner left sub image model (I_1 and I_3) is justified for partial iris image recognition. It also compares the stability of features extracted from inner right and inner left sub image model (I_1 and I_3) with the features extracted from outer right and outer left sub image model (I_5 and I_7). The extracted features from the inner right and inner left sub image model (I_1 and I_3) show greater stability as compared to the extracting features from the outer right and outer left sub image model (I_5 and I_7) even though about 25% exposed iris patterns were used to extract unique features in the inner right and inner left sub-image model (I_1 and I_3). Whereas over 35% of exposed iris patterns were utilized to extract unique features in the outer right and outer left sub-image model (I_5 and I_7). The percentage of the amount of visible iris used to extract discriminant features for partial iris image recognition is estimated for these three different kinds of partial iris image models. The Equation 3.1 is used to calculate the percentage of the iris used to extract discriminant features of the inner right and left, upper and lower partial iris image model respectively. The Equation 3.2 is used to calculate the amount of iris used in the outer right and outer left partial iris image model for recognition. Are the about 25 percent of the

visible iris in the collarette boundary of the iris good enough to extract discriminant features for partial iris image recognition? According to Daugman (University of Cambridge), the recognition can be made even by using only approximate 17 percent of the visible iris but in this case the decision criterion then becomes correspondingly more demanding.

$$\left(\frac{C-r}{R-r}\right)/2 \times 100\% \quad (3.1)$$

$$\left(\frac{R-C}{R-r}\right)/2 \times 100\% \quad (3.2)$$

where, R is the radius from the pupil centre to limbic boundary, C is the radius from the pupil centre to collarette boundary, r is the pupil radius shown in Figure 3.4 (b).

The spatial iris region I_6 and I_8 in Figure 3.2 is not used to extract features. The I_6 and I_8 regions belong to the upper and lower part of the iris image. From the intuitive observation in the iris image database, it is observed that the iris region I_6 and I_8 are occluded by the eyelids and eyelashes in maximum cases. In addition, it is also far away from the pupil boundary or collarette boundary.

3.2.1 Extracting Spatial Partial Iris Image

The three kinds of defined partial iris image models need to be transformed in the Cartesian coordinate to Polar coordinate system in this research. The polar transformation process projects different partial iris image region into a rectangular block of size so that two images of the same iris under different conditions have characteristic features at the same spatial location. This process will also help to extract scale and translation invariant features (He & Shi, 2005). Daugman's Rubber Sheet Model (Daugman, 1994, 2004) was utilized to accomplish this task. Prior to extracting different partial iris image from the different spatial

location of the iris image as described in the Figure 3.2, firstly it is needed to detect pupil boundary and the iris boundary in order to get the six parameters, the radius of the iris and pupil, and x and y centre coordinates for both iris and pupil circles are shown in Figure 3.3. Figure 3.3, (x_p, y_p) and (x_i, y_i) denote the centre coordinates of iris and pupil respectively. The most cited methods are proposed by Daugman (1994, 2004), Wildes *et al.* (1996) and Wildes (1997) to find pupil boundary and the iris boundary of the iris image (Tang *et al.*, 2009). Tang *et al.* (2009) reported that they have compared the performance of the Wildes *et al.* (1996) and Daugman (1994) algorithm in terms of accurate pupil boundary and iris boundary detection. They mentioned that they have achieved the best results using the methods proposed by Wildes *et al.* (1996) especially when image quality degraded as compared to Daugman methods. Thus, the method proposed in Wildes *et al.* (1996), Wildes (1997) and the implementation of the methods by Masek & Kovesi (2003b) were considered to accomplish this task. The details of this method are described in the Appendix I. The parameters mentioned above for the pupil boundary and iris boundary are used to unwrap defined partial iris image in the three different kinds of partial iris image models and to isolate the collarette or inner boundary and outer boundary of the iris. The collarette boundary is the edge of circle with a radius of:

$$r_c = 22 + r_p \quad (3.3)$$

where, r_c is the radius of the iris collarette boundary and r_p is the radius of the pupil boundary. In random manner, we get that by selecting a radius of 22 pixels from the edge of the pupil and the selected region usually contains the collarette region as well. The outer boundary of the iris is a circle with the edge of collarette boundary and the iris boundary of an eye image with a radius of:

$$r_o = r_i - r_c \quad (3.4)$$

where, r_o is the radius of the outer iris boundary and r_i is the radius of the iris boundary.

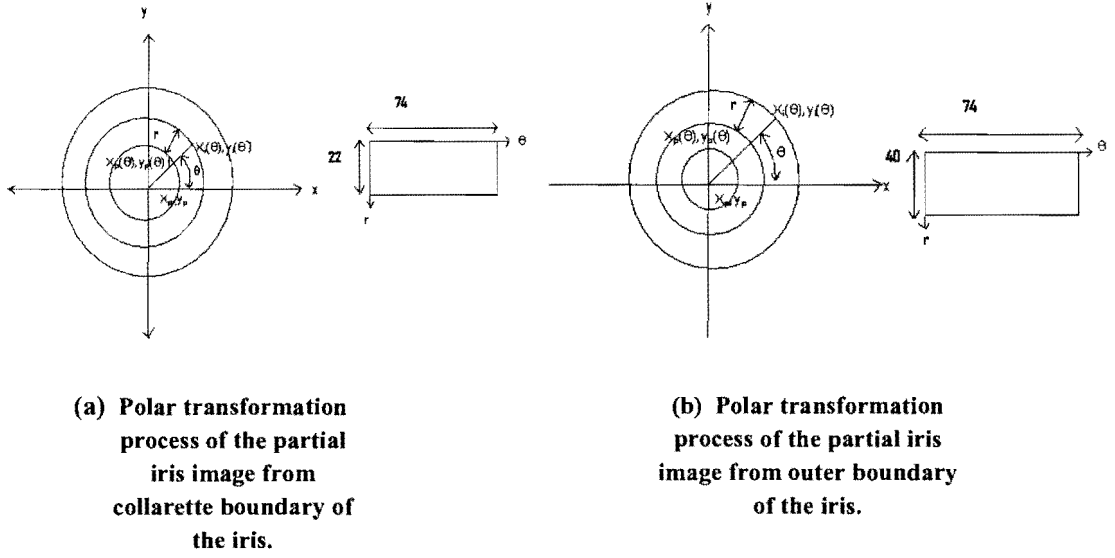
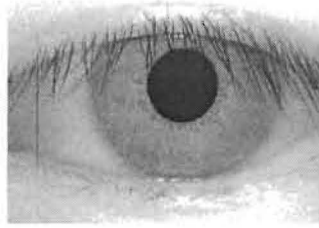
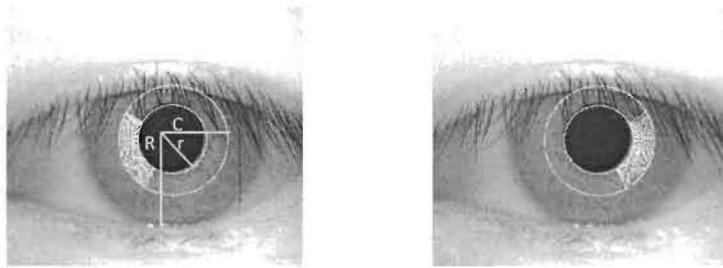


Figure 3.3 Outline of polar transformation process

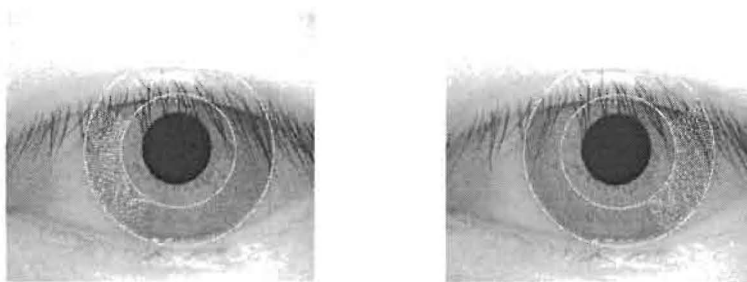
The examples of generated partial iris images both in collarette boundary and the outer boundary of the iris are shown in Figure 3.4. The shape with white stripes on the eye image represented partial sub image in the three different kinds of partial iris image model.



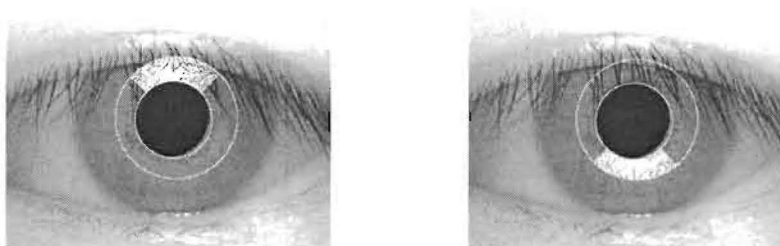
(a) Original eye image adopted from CASIA iris image database



(b) Localized collarette boundary and inner left and right sub image marks with white stripes



(c) Localized outer boundary and outer left and right sub image marks with white stripes



(d) Localized collarette boundary upper and lower sub image marks with white stripes

Figure 3.4 (a) The original eye image (b) inner right and left model (c) outer right and left model (d) upper and lower model

Size of irises from different people may be captured in different size and, even for irises from the same eye; the size may change due to the stretching of the iris caused by pupil expansion or contraction of the illumination variations and other extraneous factors that will affect the result of iris matching. Other circumstances include variance of camera and eye distance, rotation of the camera or head. It is necessary to extinguish such elastic deformation to gain accurate result (Ma *et al.*, 2003, 2004b). Hence, the defined partial iris images in Figure 3.4 are required to transform into polar coordinate system. The polar transformation process projects different partial iris image region into a rectangular block of size so that two images of the same iris under different conditions have characteristic features at the same spatial location. In this research, Daugman's Rubber sheet model (Daugman, 1994, 2004) was employed to normalize iris into a fixed size block. The Rubber sheet model formulated as follows in equation 3.5 and 3.6.

$$I(x(r, \theta), y(r, \theta)) \longrightarrow I(r, \theta) \quad (3.5)$$

Such that

$$\begin{aligned} x(r, \theta) &= (1-r) x_p(\theta) + r x_i(\theta), \\ y(r, \theta) &= (1-r) y_p(\theta) + r y_i(\theta), \end{aligned} \quad (3.6)$$

where $I(x,y)$, (x,y) , (r, θ) , $x_p(\theta)$, $y_p(\theta)$ and $x_i(\theta)$, $y_i(\theta)$ are the iris region, Cartesian coordinates, corresponding polar coordinates, coordinates of the pupil, and iris boundaries along the θ direction, respectively as shown in Figure 3.3. r is the distance from pupil boundary to collarette boundary when the inner right and inner left sub image is transformed into polar co-ordinate system as shown in Figure 3.3 (a) and Figure 3.4 (b). r is the distance from collarette boundary to iris boundary when the outer right and outer left sub images are transformed into polar co-ordinate system as shown in the Figure 3.3 (b) and 3.4 (c).

Cartesian to polar transform remaps each pixel in the iris area into a pair of polar coordinates (r, θ) , where r on the intervals $[0 \ 1]$ and angle θ are on the intervals $[-\pi/3 \ \pi/6]$ to extract and normalize inner right (I_1) and outer right (I_5) sub-image, $[5\pi/6 \ 4\pi/3]$ to extract and normalize inner left (I_3) and outer left (I_7) sub-image, $[\pi/4 \ 3\pi/4]$ and $[5\pi/4 \ 7\pi/4]$ to extract upper and lower sub image (I_2 and I_4) respectively, as described in Figure 3.2 and in Figure 3.3 from the different location of an iris image.

The dimensions of the rectangular block for the three different kinds of partial iris image models are different. It is selected based on the percentage of the iris used for each sub-image in the partial iris image model. The dimension of rectangular block 22×74 is fixed for the inner right and inner left sub-image individually in the inner right and inner left model. The Rubber Sheet Model was performed for normalization and 22 pixels along r and 74 pixels along θ were selected and got a 22×74 unwrapped strip for the inner right and inner left sub image separately. The same dimension 22×74 is fixed for the upper and lower sub image separately in the upper and lower sub image model since the percentage of the used iris in both of the partial iris image model is the same. The dimension of rectangular block 40×74 is fixed for the outer right and left sub image individually in the outer right and outer left image model. In this case the Rubber Sheet Model was performed and 40 pixels along r and 74 pixels along θ were selected and got a 40×74 unwrapped strip for the outer right and outer left sub image separately. The examples of different kinds of normalized partial iris images are shown in Figure 3.5. The normalized inner right and inner left sub images are shown in the Figure 3.5 (a). The inner right and inner left partial iris images are unwrapped from the collarette boundary of the iris that contains most useful discriminating and individually unique iris texture patterns (Ma *et al.*, 2003, 2004b; He & Shi, 2005; Roy & Bhattacharya, 2008). The inner right and inner left sub images are also safe from the occlusion by eyelids

and eyelashes, improper eye openings and other artefacts. The upper and lower sub images shown in Figure 3.5 (c) are also relying in the collarette boundary of the iris. But, it is observed that the upper and lower parts of the collarette iris region of the iris are partially covered by the eyelids and eyelashes in most of the cases which are very important source to occur false result during recognition. The normalized outer right and outer left sub image are shown in Figure 3.5 (b) that lies down far away from the pupil boundary which contains few texture characteristics and are easily occluded by eyelids and eyelashes (Ma *et al.*, 2004b).

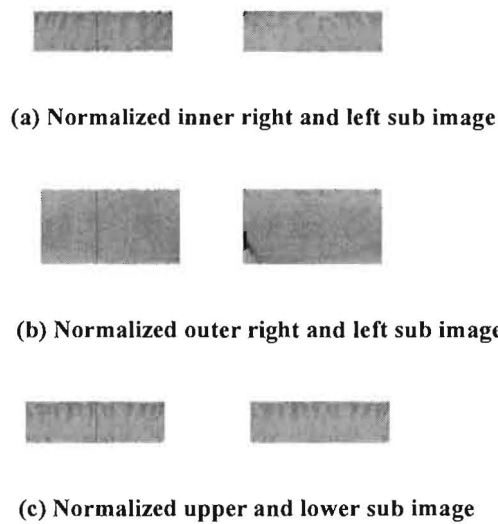


Figure 3.5 Extracted & normalized iris images for the three different kinds of partial iris image models

The illumination distribution in the polar transformed image is not uniform. The image has also low contrast. These occurrences may affect the performances of feature extraction and during the matching process. Thus in order to obtain uniform distributed illumination and better contrast in iris image, a local normalization algorithm is employed that uniformizes the local mean and variance of a polar transformed image. Contrast-limited adaptive histogram equalization Zuiderveld (1994) was applied on each partial iris images separately to enhance

polar transformed image in order to acquire the best feature for partial iris image recognition. The results of the image after enhancement are shown in the Figure 3.6.



(a) Enhanced inner right and left sub image



(b) Enhanced outer right and left iris sub image



(c) Enhanced upper and lower sub image

Figure 3.6 Enhanced iris images for the three different kinds of partial iris image models

3.3 Feature Extraction of the Partial Iris Image

The iris pattern provides abundant texture information. So, it requires a method to extract texture information in an iris. Existing feature extraction processes extract texture features from the entire iris. So, it is desirable to explore a feature extraction method which can extract local underlying information from the partial iris image. From the viewpoint of texture analysis, frequency and orientation information are mainly involved in iris texture (Ma *et al.*, 2003). Only significant information (frequency or orientation information) should be

considered as iris features. These features should be encoded, so that, comparison between templates can be made. Generally, local details of the iris spread along the radial direction in the original image corresponding to the vertical direction in the normalized image (see in Figure 1.1 and Figure 3.5). As a result, the differences of orientation information among irises are not significant (Ma *et al.*, 2003). That is, frequency information should account for the major differences of irises from different people. The wavelets transform (Daubecheis, 1988, 1992; Mallat & Hwang, 1992; Thuillard, 2001) is used to extract discriminating frequency information or characteristics values from each sub image of the different partial iris image models.

Wavelet transform is a popular approach to signal analysis and has been widely used in the field of signal and image processing since it has a fast rate as compared with a conventional signal processing algorithm based on the Fourier transform and it can efficiently accomplish signal localization in time and frequency domains (Daubecheis, 1992; Mallat & Hwang, 1992; Thuillard, 2001). When processing signals, the primary consideration is the localization, i.e., the characterization of local properties, of a given basis function in time and frequency. In this research, the signals are dealing with 2-D gray iris images, for which the time domain is the spatial location of certain gray pixels and the frequency domain is the texture variations around a pixel. Thus, it is needed to seek for a suitable method that can effectively represent the texture variations in each spatial region of the partial iris image.

The method of extracting the iris features and forming the feature vector use in the conventional iris recognition field are Gabor filters (Daugman, 1993, 2003, 2004). But, the outputs of Gabor filter banks are not mutually orthogonal, which may result in a significant correlation between texture features. Finally, these transformations are usually not reversible,

which limits their applicability for texture synthesis. Most of these problems can be avoided if one uses the wavelet transform, which provides a precise and unifying framework for the analysis and characterization of a signal at different scales (Unser, 1995). Another advantage of wavelet transform over Gabor filters is that the low-pass and high-pass filters used in the wavelet transform remain the same between two consecutive scales while the Gabor approach requires filters of different parameters (Chang & Kuo, 1993). In other words, Gabor filters require proper tuning of filter parameters at different scales (Arivazhagan & Ganesan, 2004). The other weakness of the Gabor filter is the even symmetric filter will have a DC component whenever the bandwidth is larger than one octave (Field, 1987) that means DC component may affect of the computed iris code by the strength of illumination due to DC response in real parts of the filtered image. The characteristics vectors generated by these methods are formed to have 256 or more dimensions, and they require at least 256 bytes even though it is assumed that one byte is assigned to one dimension.

A Laplacian pyramid is constructed with four different resolution levels in Wildes *et al.* (1996), Wildes (1997) in order to generate a compact iris image data. The Laplacian pyramid data structures suffer from the difficulty that data at separate levels are correlated. There is no clear model which handles this correlation. It is thus difficult to know whether a similarity between the image details at different resolutions is due to a property of the image itself or to the intrinsic redundancy of the representation. Furthermore, the Laplacian multi-resolution representation does not introduce any spatial orientation selectivity into the decomposition process. This spatial homogeneity can be inconvenient for pattern recognition problems such as texture discrimination (Mallat, 1989).

Haar wavelet transform has been widely used in conventional iris recognition (Kim *et al.*, 2001), image processing and the like. Haar found an orthonormal base defined on $[0, 1]$, namely $h_0(x), h_1(x), \dots, h_n(x), \dots$, such that for any continuous function $f(x)$ on $[0, 1]$, the series

$$\sum_{j=1}^{\infty} \langle f, h_j \rangle h_j(x) \quad (3.7)$$

converges to $f(x)$ uniformly on $[0, 1]$. Here, $\langle u, v \rangle$ denotes $\int_0^1 u(x) \overline{v(x)} dx$ and \bar{v} is the complex conjugate of v . One version of Haar's construction (Wang *et al.*, 1998) can be written as follows:

$$h(x) = \begin{cases} 1 & x \in [0, 0.5) \\ -1 & x \in [0.5, 1) \\ 0 & \text{elsewhere} \end{cases} \quad (3.8)$$

$$h_n(x) = 2^{j/2} h(2^j x - k) \quad (3.9)$$

where $n = 2^j + k$, $k \in [0, 2^j]$, $x \in [k2^{-j}, (k+1)2^{-j}]$.

There are problems with Haar's construction. For example, Haar's base functions are discontinuous step functions and are not suitable for analyzing continuous functions with continuous derivatives. If the images considered as 2-D continuous surfaces, Haar's base functions are not appropriate for image analysis (Vetterli & Herley, 1992; Wang *et al.*, 1998). Thus, Haar wavelet functions have disadvantages that the characteristic values are discontinuous and rapidly changing and that high resolution of the images cannot be obtained in a case where the images are again decompressed after they have been compressed.

Another basis for wavelet is that of Daubechies. For each integer r , Daubechies orthonormal basis (Daubechies, 1988, 1992; Thuillard, 2001) for $L^2(R)$ is defined as:

$$\phi_{r,j,k}(x) = 2^{j/2} \phi_r(2^j x - k), \quad j, k \in \mathbb{Z} \quad (3.10)$$

where the function $\phi_r(x)$ in $L^2(R)$ has the property that $\{\phi_r(x-k) \mid k \in \mathbb{Z}\}$ is an orthonormal sequence in $L^2(R)$. Then, the trend f_j , at scale 2^{-j} , of a function $f \in L^2(R)$ is defined as

$$f_j(x) = \sum_k \langle f, \phi_{r,j,k} \rangle \phi_{r,j,k}(x) \quad (3.11)$$

The details or fluctuations are defined by

$$d_j(x) = f_{j+1}(x) - f_j(x) \quad (3.12)$$

To analyse these details at a given scale Daubechies ortho-normal basis $\psi_r(x)$ is defined and it is having properties similar to those of $\phi_r(x)$ described above. $\phi_r(x)$ and $\psi_r(x)$, called father wavelet and the mother wavelet, respectively. Daubechies orthonormal basis has the following properties (Wang *et al.*, 1998)

ψ_r has the compact support interval $[0, 2r+1]$

ψ_r has about $r/5$ continuous derivatives

$$\int_{-\infty}^{\infty} \psi_r(x) dx = \dots = \int_{-\infty}^{\infty} x^r \psi_r(x) dx = 0$$

Daubechies wavelets give remarkable results in image analysis and synthesis due to the above properties (Wang *et al.*, 1998). In fact, a wavelet function with compact support can be easily implemented by finite length filters. This finite length property is important for spatial domain localization. Furthermore, functions with more continuous derivatives analyze continuous

functions more efficiently and avoid the generation of edge artefacts. Since the mother wavelets are used to characterize details in the signal, they should have a zero integral so that the trend information is stored in the coefficients obtained by the father wavelet. A Daubechies wavelet representation of a function is a linear combination of the wavelet function elements.

The Daubechies DB8 discrete wavelet transform is generated in this research to extract discriminating frequency information or characteristics values from each sub image of the different partial iris image models, and it is a kind of technique of analysing signals in multi-resolution mode. The Daubechies wavelet functions (Daubechies, 1988, 1992) are continuous functions. The disadvantages of the Haar wavelet functions that the values thereof are discontinuous and rapidly changing can be avoided, and the characteristics values can be extracted more accurately. Therefore, in case where the images are to be again decompressed after they have been compressed by using the Daubechies wavelet transform, the images can be restored in high resolution nearer to the original images than the Haar wavelet transform is used. The Daubechies wavelet transform also reduces the dimension of the characteristics vector.

A discrete wavelet transform (DWT) maps the time-domain signal of $f(t)$ into a real valued time-frequency domain and the signals are described by the wavelet coefficients. Since, coefficients of the filtered image effectively indicate the frequency distribution of an image (Ma *et al.*, 2003). Suppose that a signal $f(t)$ is already in the approximation space V_j , that is:

$$f(t) = \sum_{k \in \mathbb{Z}} a_k^{-j} \varphi(2^j t - k) \in V_j \quad (3.13)$$

Then, the decomposition of this signal to the next level can be written as (Manjunath & Ravikumar, 2010)

$$f(t) = \sum_{k \in \mathbb{Z}} a_k^{j-1} \varphi(2^{j-1}t - k) + \sum_{k \in \mathbb{Z}} d_k^{j-1} \psi(2^{j-1}t - k) \quad (3.14)$$

where a_k^j are the approximation coefficients which represent the smoothed part of the signal, and the d_k^j are the detail coefficients. In practice, 2-D discrete wavelets transform is computed by applying a separable filter bank to the image

$$L_n(i, j) = [L_x * [L_y * L_{n-1}] \downarrow 1, 2] \downarrow 2, 1(i, j)$$

$$D_{n1}(i, j) = [L_x * [H_y * L_{n-1}] \downarrow 1, 2] \downarrow 2, 1(i, j)$$

$$D_{n2}(i, j) = [H_x * [L_y * L_{n-1}] \downarrow 1, 2] \downarrow 2, 1(i, j)$$

$$D_{n3}(i, j) = [H_x * [H_y * L_{n-1}] \downarrow 1, 2] \downarrow 2, 1(i, j)$$

where $*$ denotes the convolution operator, $\downarrow 2, 1(\downarrow 1, 2)$ denotes sub sampling along the rows (columns), and L_0 is the original image. L and H are the low-pass and high-pass filter, respectively. L_n is obtained by low-pass filtering and is therefore referred to as the lower resolution image at scale n . The detailed images of $D_{n,i}$ are obtained by band-pass filtering in a specific direction and contain directional detail information at scale n . The original image I is thus represented by a set of sub images at several scales: $\{L_d, D_{n,i}\}_{i=1,2,3, n=1,2,\dots,d}$, which is a multi-scale representation of depth d of the image I (Wouwer *et al.*, 1999). Figure 3.7 shows an example of multi-dividing partial iris image by applying Daubechies DB8

discrete wavelet transform. Analysis of iris textures requires the identification of proper attributes or features that differentiate the textures in the image for partial iris recognition. Traditionally, the texture components in the image have high frequency spectrum (Sivabalan & Ghanadurai, 2010). Spatial information is of critical importance in high frequency bands than that of lower frequency bands of the wavelet transformed image (Lakshmi & Rakshit, 2010). Thus, in order to extract discriminant features or characteristics values, the Daubechies DB8 discrete wavelet transform is repeatedly performed of each sub image in the different partial iris image models for predetermined number of times and extract the image including the high frequency components from the multi-divided image so as to extract iris features for each sub images.

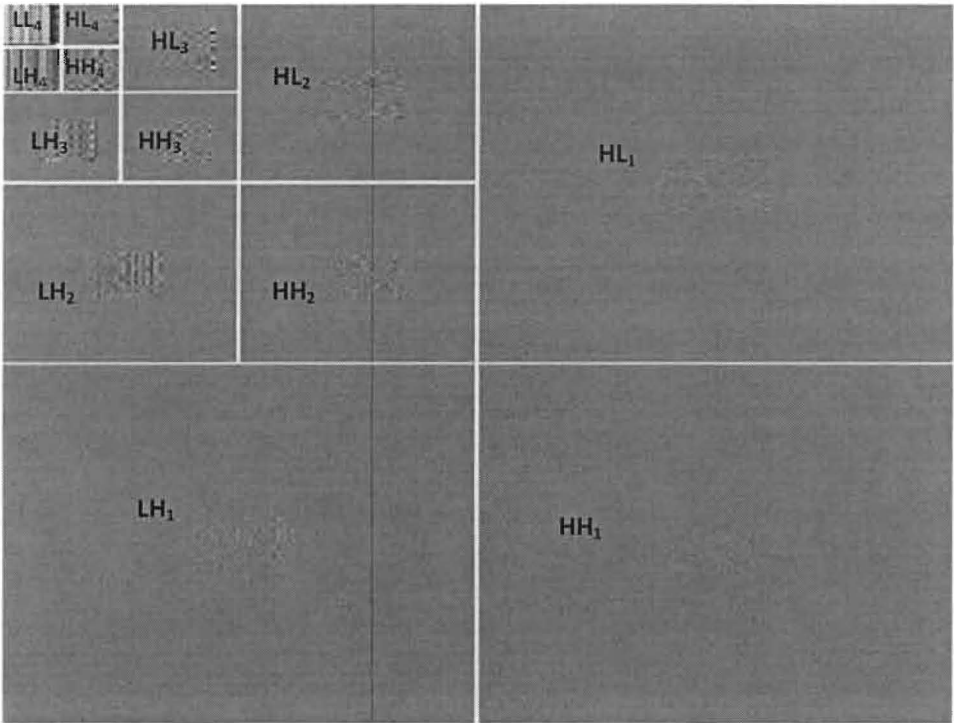


Figure 3.7 A 4-level wavelet decomposition procedure using DB8 wavelets

The Daubechies wavelet function with Db4-Db16 coefficients has been investigated. The more discriminating characteristics values is achieved by using wavelet functions with eight coefficients DB8 rather than the Daubechies wavelet transform with wavelet functions less or more than eight coefficients. Although, the Daubechies wavelet function with more than eight coefficients can extract more sensitive characteristics values, but the greater performance improvement was not achieved rather, processing time is increased compared to the case where the Daubechies wavelet function with eight coefficients. This guides to apply the Daubechies wavelet function with eight coefficients DB8 to extract discriminating characteristics values of the each sub image in the different partial iris image models. The filters associated with DB8 are as illustrated in Table II.

Table II The low-pass and high-pass filters of DB8

	Low-pass filter	High-pass filter
1.	-0.0001	-0.0544
2.	0.0007	0.3129
3.	-0.0004	-0.6756
4.	-0.0049	0.5854
5.	0.0087	0.0158
6.	0.0140	-0.2840
7.	-0.0441	-0.0005
8.	-0.0174	0.1287
9.	0.1287	0.0174
10.	0.0005	-0.0441
11.	-0.2840	-0.0140
12.	-0.0158	0.0087
13.	0.5854	0.0049
14.	0.6756	-0.0004
15.	0.3129	-0.0007
16.	0.0544	-0.0001

The multi-resolution partial iris image by performing Daubechies DB8 discrete wavelet transform is shown in the Figure 3.7. In the Figure 3.7, “L” and “H” are used to indicate low frequency and high frequency components, respectively. The term ‘LL’ means a component

that has passed through a low pass filter (LPF) in all x- and y- directions whereas a term 'HH' means a component that has passed through a high-pass filter (HPF) in the x- and y- directions. For example, 'HL₂' means that the image has passed through the high pass filter in the x- direction and through the low pass filter in the y- direction during 2-stage wavelet division. The iris image is considered as a two-dimensional signal in which one-dimensional signals are arrayed in the x- and y- directions, quarterly divided components of one image should be extracted by passing through the low pass filter (LPF) and high pass filter (HPF) in all x- and y- directions in order to analyse the each sub image in the partial iris image model. That is, a two-dimensional image signal is wavelet transformed in horizontal and vertical directions, and the image is divided into four regions 'LL', 'HL', 'LH' and 'HH' after the wavelet transform has been performed once. At this time, the signal is divided into a differential component thereof that has passed through the high pass-filter, and an average component that has passed through the low pass filter through Daubechies wavelet transform. The 'LL' region contains only low frequency components in the x- and y- directions in the multi-divided iris image. Since the extracted region 'LL' includes major information on the iris image, it is provided as an image to be newly processed so that the wavelet transform can be again applied to the relevant region. Then, the Daubechies DB8 discrete wavelet transform is repeatedly performed in order to reduce the information sizes. In this way, the characteristics values of further reduced regions HH₄ is obtained. The iterative number, which is provided as a discriminating criterion for repeatedly performing the wavelet transform, should be set as a proper value in consideration of the loss of the information and the size of the characteristics vector. In the experiment, this value is fixed up with 4. Therefore, in this research, the region HH₄ of each sub images in the partial iris image model is obtained by performing the wavelet transform four times which is considered as a major characteristics

region. The values of HH₄ region of each sub images in the different partial iris image models is considered as components of the characteristics vector. The high frequency components extracted from the HH₄ region of the wavelet transformed image provide better discrimination among the iris images in the database. The frequency information (coefficients of the wavelet transformed image) of the wavelet transformed image in different (1 to 4) level is also investigated but, the most discriminant features is achieved by extracting only high frequency components at the 4th level of the wavelet transformed image. After extraction of the characteristics of each sub image signals in the three different kinds of partial iris image models has been completed, the characteristics vector is generated based on these extracted characteristics.

3.3.1 Characteristics Vector Generation

The characteristics vector is generated for the three different kinds of partial iris image models individually. i.e., the three characteristics vector is generated for each individual iris image in the database for the three different kinds of partial iris image models. Then, the three characteristics vector of each individual iris image in the database is encoded to binary feature vector representation. Several experiments are performed among the iris images in the database based on these generated feature vectors for the three different kinds of partial iris image models in order to evaluate the stability of the extracted features and to find out the stable region on the iris for partial iris recognition. The extracted characteristics values from the region HH₄ of each sub images in the different partial iris image models is considered as components of the characteristics vector. The region HH₄ contains high frequency information of 270 (=15×18) data for each inner right and inner left sub images of the inner right and inner left partial iris image model. All the characteristics values obtained on the regions HH₄ for each inner right and inner left sub images of the inner right and inner left

partial iris image model is concatenated to make a unique characteristics vector for each of the iris images in the CASIA iris image database. The same procedure is applied to form the individually unique characteristics vector with extracted high frequency components from the HH₄ regions of the wavelet transformed image for the outer right and outer left, upper and lower partial iris image models respectively. The characteristics vector F is obtained for the inner right and inner left partial iris image model using equation (3.15). F is the characteristics vector where, f^{ir} is the extracted characteristics information of the inner right sub-image and f^{il} is the extracted characteristics information of the inner left sub-image in the inner right and inner left partial iris image model.

$$F = \{f^{ir}, f^{il}\} \quad (3.15)$$

where,

$$f^{ir} = \begin{bmatrix} f_{1,1} & f_{1,2} & f_{1,3} & \cdots & f_{1,18} \\ f_{2,1} & f_{2,2} & f_{2,3} & \cdots & f_{2,18} \\ \vdots & \vdots & \vdots & \cdots & \vdots \\ \vdots & \vdots & \vdots & \cdots & \vdots \\ f_{15,1} & f_{15,2} & f_{15,3} & \cdots & f_{15,18} \end{bmatrix}, \text{ and}$$

$$f^{il} = \begin{bmatrix} f_{1,1} & f_{1,2} & f_{1,3} & \cdots & f_{1,18} \\ f_{2,1} & f_{2,2} & f_{2,3} & \cdots & f_{2,18} \\ \vdots & \vdots & \vdots & \cdots & \vdots \\ \vdots & \vdots & \vdots & \cdots & \vdots \\ f_{15,1} & f_{15,2} & f_{15,3} & \cdots & f_{15,18} \end{bmatrix}$$

The total number of $(2 \times 270) = 540$ characteristics values obtained after concatenated of the extracted high frequency components from the inner right and inner left partial iris image model. The region HH₄ contains high frequency information of 288 ($=16 \times 18$) data for each outer right and outer left sub images of the outer right and outer left partial iris image model.

The characteristics vector F_I is obtained for the outer right and outer left partial iris model using equation (3.16). F_I is the characteristics vector where, f^{or} is the extracted characteristics information of the outer right sub-image and f^{ol} is the extracted characteristics information of the outer left sub-image in the outer right and outer left partial iris image model.

$$F_I = \{f^{or}, f^{ol}\} \quad (3.16)$$

$$\text{where, } f^{or} = \begin{bmatrix} f_{1,1} & f_{1,2} & f_{1,3} & \cdots & f_{1,18} \\ f_{2,1} & f_{2,2} & f_{2,3} & \cdots & f_{2,18} \\ \vdots & \vdots & \vdots & \cdots & \vdots \\ \vdots & \vdots & \vdots & \cdots & \vdots \\ f_{16,1} & f_{15,2} & f_{15,3} & \cdots & f_{16,18} \end{bmatrix}, \text{ and}$$

$$f^{ol} = \begin{bmatrix} f_{1,1} & f_{1,2} & f_{1,3} & \cdots & f_{1,18} \\ f_{2,1} & f_{2,2} & f_{2,3} & \cdots & f_{2,18} \\ \vdots & \vdots & \vdots & \cdots & \vdots \\ \vdots & \vdots & \vdots & \cdots & \vdots \\ f_{16,1} & f_{15,2} & f_{15,3} & \cdots & f_{16,18} \end{bmatrix}$$

The total number of $(2 \times 288) = 576$ characteristics values obtained after concatenated of extracted high frequency components from the outer right and outer left partial iris image model. The region HH4 contains high frequency information of 270 ($=15 \times 18$) data for each upper and lower sub images of the upper and lower partial iris image model. The characteristics vector F_2 is obtained for the upper and lower partial iris image model using equation (3.17). F_2 is the characteristics vector where, f^u is the extracted characteristics information of the upper sub-image and f^l is the extracted characteristics information of the lower sub-image in the upper and lower partial iris image model.

$$F_2 = \{f^u, f^l\} \quad (3.17)$$

where, $f^u = \begin{bmatrix} f_{1,1} & f_{1,2} & f_{1,3} & \cdots & f_{1,18} \\ f_{2,1} & f_{2,2} & f_{2,3} & \cdots & f_{2,18} \\ \cdot & \cdot & \cdot & \cdots & \cdot \\ \cdot & \cdot & \cdot & \cdots & \cdot \\ \cdot & \cdot & \cdot & \cdots & \cdot \\ f_{15,1} & f_{15,2} & f_{15,3} & \cdots & f_{15,18} \end{bmatrix}$, and

$$f^l = \begin{bmatrix} f_{1,1} & f_{1,2} & f_{1,3} & \cdots & f_{1,18} \\ f_{2,1} & f_{2,2} & f_{2,3} & \cdots & f_{2,18} \\ \cdot & \cdot & \cdot & \cdots & \cdot \\ \cdot & \cdot & \cdot & \cdots & \cdot \\ \cdot & \cdot & \cdot & \cdots & \cdot \\ f_{15,1} & f_{15,2} & f_{15,3} & \cdots & f_{15,18} \end{bmatrix}$$

The total number of $(2 \times 270) = 540$ characteristics values obtained after concatenated of the extracted high frequency components from both of the sub image in the upper and lower partial iris image model. A module for generating the characteristics vector mainly performs the processes of extracting the characteristics values in the form of real numbers and then transforming them to binary codes consisting of 0 and 1.

3.3.2 Binary Feature Vector Representation

The binary feature vector is generated for unique feature vector representation. The characteristics vector is converted into binary feature vector so that utility of human partial iris recognition can be improved by reducing storage capacity and processing time. The binary feature vector is generated by quantizing the relevant characteristics values of a characteristics vector from the extracted image including high frequency components or characteristics values in the fourth level of wavelet transformed image. In the previous section, the characteristics vector is obtained of 540 components for the inner right and inner

left and upper and lower partial iris image model respectively. The characteristics vector of 576 components is obtained for the outer right and outer left partial iris image model. The extracted characteristics values distribution of a partial iris image illustrates in Figure 3.8. Since, each component of characteristics vectors has a real value lie in the range of -1.5 to +1.5, the characteristics vector is sign quantized (Kim *et al.*, 2001) so that any positive value is represented by 1 and negative value as 0. Boles & Boashash (1998) decomposed an entire iris image using dyadic wavelet filters and then selected only the number of zero-crossing as features. But, in case of partial iris image this method is not suitable because the size of partial iris image is smaller rather than entire iris image. Thus, the number of zero crossing will be decreased predominantly if this technique is applied to partial iris image. The lowest number of zero-crossing information may not be enough to produce discriminant features for partial iris image recognition. The problem of this method is that the number of zero-crossing can differ among iris image samples of an identical iris due to noises (Kim *et al.*, 2006).

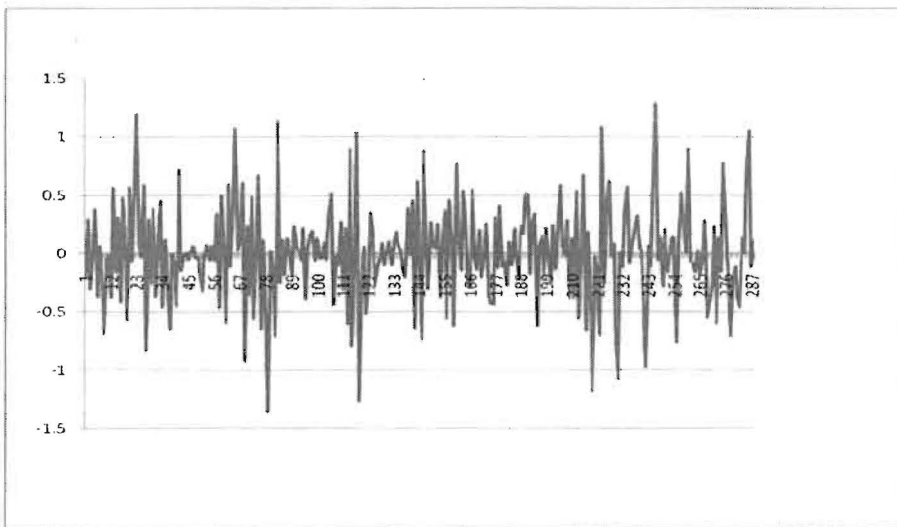


Figure 3.8 The extracted characteristics values distribution of a partial iris image

The following algorithm is used for conversion the characteristics vector into binary feature vector.

If $\text{Coeff}(i) \geq 0$ then $\text{Coeff}(i) = 1$;

If $\text{Coeff}(i) < 0$ then $\text{Coeff}(i) = 0$;

$\text{Coeff}(i)$ is one of the elements of characteristics vector. The binary 1 is chosen if the corresponding element in the characteristics vector is greater than or equal to zero and binary 0 is selected if the element is less than zero or negative. In this way, the binary feature vector is made which was comprised of 540 bits for the inner right and inner left partial iris image model and upper and lower partial iris image model respectively. Whereas, the binary feature vector of 576 bits for the outer right and outer left partial iris image model. The generated two feature vectors of inner right and inner left partial iris image model and outer right and outer left partial iris image models are shown in the Figure 3.9. The binary feature vectors are generated as described in Figure 3.9 for the three different kinds of partial iris image models of each individual in the CASIA iris image database. Then, these feature vectors have been used for training and testing in order to validate the stability of the extracted iris features and derive the stable region on the iris for partial iris recognition.

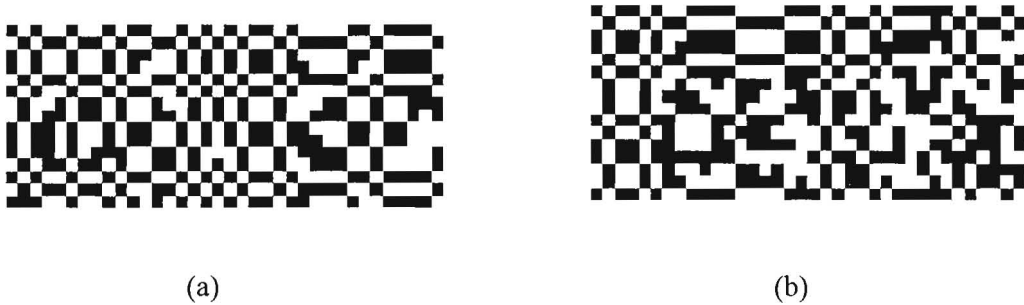


Figure 3.9 (a) Feature vector with 540 bits for inner right and left partial iris image model (b) feature vector with 576 bits for outer right and outer left partial iris image model

3.4 Feature Matching and Distance Measure

In the matching stage, it is decided whether the iris images are from the same class or not through a comparison between the corresponding feature vectors of two irises. In this research, the matching process will be fast and simple since the feature vector is in binary. The different similarity measurement techniques have been described in Chapter 2. Among these similarity measurement technique used is the Hamming Distance (HD) technique (Daugman, 2004) that is generated to measure the similarities among the templates. The most favored distance measure is the Hamming distance when the features are binary (Cha *et al.*, 2006). In this research, the binary feature vector is generated and thus Hamming distance similarity measurement technique has been used to compare the templates or feature vectors generated from the three different kind of partial iris image models in the CASIA iris image database. The other similarity measurement techniques have not been considered in this research since these techniques were used when the templates or features are composed of integer values (Masek, 2003a). Hamming Distance (HD) is calculated by total number of dissimilar bits that is divided by total number of compared bits between the two templates which is to be compared.

$$HD = \frac{1}{MN} \sum_{i=1}^M \sum_{j=1}^N F_A(i, j) \text{ XOR } F_B(i, j) \quad (3.18)$$

where F_A and F_B are the feature vector of two iris images and $M \times N$ is the size of the feature vector. The XOR is the known Boolean operator that gives a binary 1 if the bits at position (i, j) in F_A and F_B are different and 0 if they are similar.

It is expected to get a partial iris representation invariant to translation, scale and rotation. In this research, translation and scale invariance are achieved by normalizing the original image at the partial iris image requirement step. Existing approaches (Daugman, 1993, 1994, 2001a, 2001b, 2004; Masek, 2003a) used shift in the iris code in order to achieve rotation invariant feature vector before matching. In this research, no shifts in the iris code were used. As results achieved are without any shifts in the iris templates that speed up the matching process to a considerable extent.

3.5 Evaluation Methods

In order to assess the performance of the feature extraction method for partial iris image recognition, the experiments are done by extracting features through three different kinds of partial iris image models separately. The intra-class and inter-class distances are calculated among the templates or feature vectors in the database. When comparing templates (feature vectors) are generated from the same eye known as intra-class comparisons. On the other hand, comparing the templates generated from the different eyes is known as inter-class comparison (Gawande *et al.*, 2010). The Hamming distance similarity measurement technique has been used to calculate the intra-class and inter-class distance as details described in the previous section. Then, the intra-class and inter-class distances have been observed in order to make a decision criterion. The proposed algorithm was tested in verification mode in order to achieve the accuracy of the proposed method. In verification mode, assuming that a test sample is from a specified subject and the performance is measured in terms of three error rates: False Accept Rate (FAR), False Reject Rate (FRR) and Equal error rate (EER) (Prabhakar *et al.*, 2003), (Jain *et al.*, 2004), (Anon, 2008) from the intra-class and inter-class distance distribution to evaluate the accuracy of the proposed

feature extraction method of the partial iris recognition. FAR and FRR describe the rates of the two types of error related to decision threshold. The FAR is the probability of accepting an imposter as a genuine user and the FRR is the probability of a genuine user being incorrectly rejected. For every score value (Hamming distance) i on range (0.0, 1.0) the following functions are created.

- False Acceptance Rate (FAR (i)): The FAR value for score i (DT) is the number of imposter comparisons with score lower than i divided by the total number of imposter comparison.
- False Rejection Rate (FRR (i)): The FRR value for score i (DT) is the number of genuine comparisons with score higher than i divided by the total number of genuine comparison.
- Equal Error Rate (EER): EER is the value where FAR (i) and FRR (i) are equal, i.e., where $\text{FAR}(i) = \text{FRR}(i)$.

The EER is the best single description of the Error Rate of an algorithm and as lower be the EER the lower error rate of the algorithm (Anon, 2008).

3.6 Summary

At the beginning of this chapter, the image requirement for partial iris recognition is described. Based on study and analysis in the CASIA iris image database, the three different partial iris image models are designed. Then, the designing of the method in order to unwrap partial iris image from the different location of the iris is explained to get translation and scale invariant features. The overall design of a new feature extraction method for partial iris image recognition is explained in detail. This design explained how different wavelet filters applied

to the unwrapped partial iris image and how a set of sub images are obtained at different resolution levels. This design also explained how to select features from the different levels of the wavelet transformed image and the reasons of using these features are also explained. From the extracted features it is also explained how to construct feature vector for the three different kinds of partial iris image models of each individual subject in the database. The Hamming distance similarity measurement technique is described in order to classify among the extracted templates for the three different kinds of partial iris image models in the database. The training and testing results with the Hamming distance classifier are described in detail in Chapter 4 in order to justify the stability of the features extracted through the proposed method. Lastly, several evaluation methods have been described in order to assess the performance of the feature extraction method for partial iris image recognition.

Chapter 4 Experiments and Results Analysis

4.1 Introduction

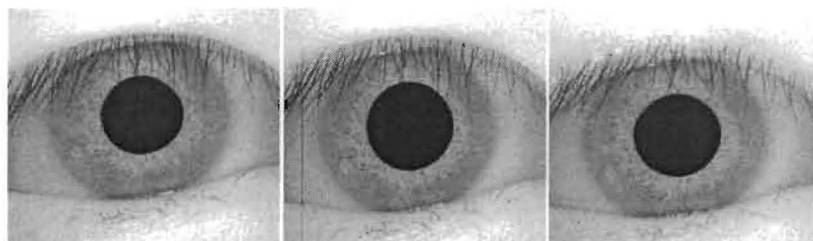
This chapter discusses results and analysis in order to evaluate the performance of the proposed feature extraction method and to derive the stable region on the iris for partial iris recognition. The performance of the proposed feature extraction method is evaluated by extracting features of the different partial iris image models as explained in Chapter 3. The experiments have been accomplished separately by extracting features of the three different kinds of partial iris image models. Firstly, the experiment is done by extracting features through inner right and inner left partial iris image models in the database. The intra-class and inter-class distances are calculated among the templates or feature vectors in the database. The Hamming distance similarity measurement technique has been used to calculate the intra-class and inter-class distances as described in detail in Chapter 3. Then, the intra-class and inter-class distances have been observed in order to make a decision criterion. The same procedures are followed for the outer right and outer left, upper and lower partial iris image models respectively.

A comparative analysis has been performed on the results produced by the intra-class and inter-class comparison based on the extracted features of the three different kinds of partial iris models in the database. Finally, the performance is measured in terms of three error rates: False Accept Rate (FAR), False Reject Rate (FRR) and Equal error rate (EER) from the intra-class and inter-class distance distribution to evaluate the accuracy of the proposed feature extraction method of the partial iris recognition. The process of evaluating not only shows the stability of the extracted features for partial iris recognition but also derive the stable region of the iris for partial iris recognition.

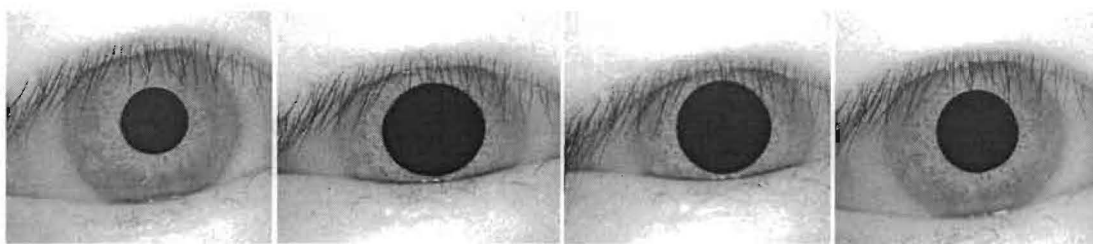
4.2 The Sample Database

There are some datasets available in the field of iris recognition in recent times such as UBath, MMU, and CASIA version 1.0 to version 4.0 iris image databases. The UBath database (University of Bath Iris Image Database, 2007) is constructed with a machine vision camera under NIR illumination. The quality of iris images in UBath iris image database is good because of controlled capture interface, illumination, and cooperative volunteers (Sun & Tan, 2009) similar to the images from MMU iris database (Multimedia University Iris Image Database). Among the CASIA version 1.0 to CASIA version 4.0 iris image databases, CASIA version 1.0 iris image database contains non-ideal images (Xu *et al.*, 2006). Dorairaj *et al.* (2005) also reported that the images in CASIA version 1.0 dataset are strongly occluded and defocused. Hence, the proposed approach has been tested with (CASIA-Iris Image Databases Version 1.0 (CASIA-IrisV1)) in order to evaluate the performance of the proposed feature extraction method and to find out the stable region of the iris for partial iris recognition that includes 756 images from 108 different eyes or subjects. For each eye, 7 images are captured in two sessions, where three samples are collected in the first session and four in the second session. The size of the each iris images in the database is 320×280 . As it is known that, the time lag between the date when the images are captured for user enrollment and the date when the test images are taken has an effect on intra-class matching distances since there may be great variations between images of the same iris taken at different times due to changes of imaging conditions. The iris samples from CASIA Iris Image Databases are shown in Figure 4.1 and from there it is observable that the variations between images of the same iris taken at different session. Among the iris images taken at the second session shown in Figure 4.1(b), pupils of the iris are dilated; images are occluded by the eyelids and eyelashes, more illuminated as compared to the images taken at the first session of the same eyes shown in

Figure 4.1(a) and these factors mentioned above degrade the recognition performance. Thus, in order to explore the impact of the time lag, three samples were taken at the first session used for training and all samples captured at the second session served as test samples for each iris subjects. The images were taken especially for iris image recognition research using specialized digital optics – a homemade digital camera which was used to capture the iris database developed by the National Laboratory of Pattern Recognition, China (CASIA-Iris Image Databases Version 1.0 (CASIA-IrisV1)). The images were mainly from samples of Asian descent, whose eyes are characterized by irises that are densely pigmented, and with dark eyelashes. Due to specialized imaging conditions using near-infrared light, features in the iris region are highly visible and there is good contrast between pupil, iris and sclera regions. This is also consistent with the widely accepted standard for iris biometrics algorithm testing (CASIA-Iris Image Databases Version 1.0 (CASIA-IrisV1); Xu *et al.*, 2006)).



(a) Iris image taken from the first session



(b) Iris image taken from the second session

Figure 4.1 Iris samples from CASIA iris image databases (a) iris image taken from the first session for training (b) iris image taken from the second session for testing

4.3 Performance Evaluation of the Feature Extraction Method for Partial Iris Image Recognition

In order to assess the performance of the feature extraction method for partial iris image recognition, firstly the experiment is done by extracting features through inner right and inner left partial iris image models in the database. The extracted features of the inner right and inner left partial iris image models are stored as feature vector for every individual iris image in the database. Firstly, the Intra-class and Inter-class comparisons are performed among the extracted templates or feature vectors of the inner right and inner left partial iris image models in the CASIA iris image database. Comparing the templates generated from the same eye known as intra-class comparison and comparing the templates generated from different eyes known as inter-class comparison. The same procedure is followed to evaluate the extracted features of the outer right and outer left, upper and lower partial iris image models respectively.

The images of the same iris taken at different sessions may be effecting on intra-class matching distances since there may be variations between images of the same iris. In order to explore the impact of this variation on the features extracted through the proposed feature extraction method for partial iris recognition, the experimental results were analyzed separately based on comparisons between images taken at the same session and those based on comparisons between images taken at different session. The numbers of quantitative intra-class and inter-class comparisons performed are shown in Table III, IV, V and VI respectively. In CASIA iris database, the time lag between different capture sessions was at least one month. For the results from comparing images taken at the same session, the distribution of intra-class matching distance is judged with 324 comparisons among 108

individual iris images and inter-class matching distance distribution is calculated with 7350 comparisons among 50 individual iris images for the three different kinds of partial iris image models. The distributions of matching distance for the different kinds of partial iris image models are shown in the Figure 4.2, 4.3 and 4.4. In this research, the experiments were carried out by comparing images taken at different session only for the templates extracted from the inner right and inner left partial iris image models and in this case the distribution of intra-class matching distance is judged with 600 comparisons among 50 individual iris images and inter-class matching distance that is counted on 588 comparisons among 58 individual iris images.

Table III Intra-class comparisons for images taken at the same session

Number of individual iris images	Number of iris images of each individual	Number of comparisons performed
108	3	324

Table IV Inter-class comparisons for images taken at the same session

Number of individual iris images	Number of iris images of each individual	Number of comparisons performed
50	3	7350

Table V Intra-class comparisons for images taken at the different session

Number of individual iris images	Number of iris images of each individual	Number of comparisons performed
50	3×4	600

Table VI Inter-class comparisons for images taken at the different session

Number of individual iris images	Number of iris images of each individual	Number of comparisons performed
50	3×4	588

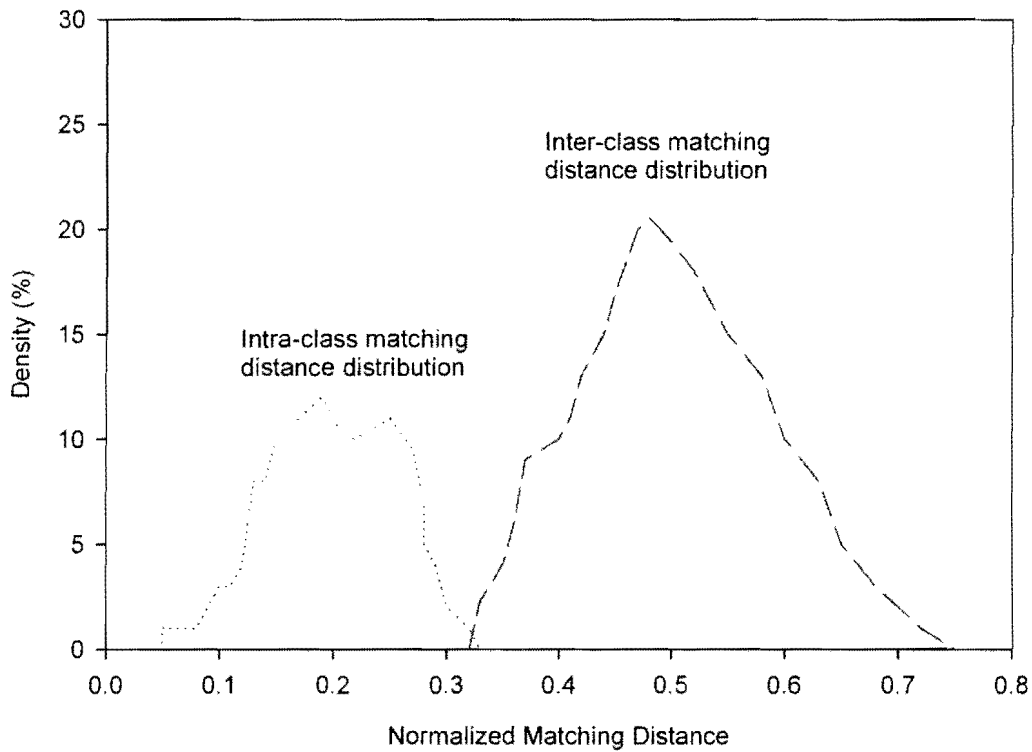












Figure 4.2 Distribution of intra-class and inter-class distances for the templates extracted from the inner right and inner left partial iris image models











The normalized matching distance distribution for the feature vector (templates) generated from the inner right and inner left partial iris image model is illustrated in Figure 4.2. Figure 4.2 shows that the fractional Hamming distance always relies between 0.05 to 0.33 during intra-class comparisons with templates extracting from the inner right and inner left partial iris image model for all the iris images in the CASIA iris image database that was taken in the first session. On the other hand, it is observed that the fractional Hamming distance increases substantially during inter-class comparison or comparison with unrelated iris templates and in





this case fractional Hamming distance always relies between 0.33 to above 0.7. This separation between intra-class (same class) and inter-class distances (different class) distribution show better discrimination power of the features extracted from the inner right and inner left partial iris image model. Table VII depicts the process of intra-class and inter-class Hamming distance distribution in the database during comparisons with the templates extracted from the inner right and inner left partial iris image model. Syntax is XXX \ S \ XXX_S_Y.bmp where XXX is the unique identifier of the eye, S is the index of the session, and Y is the index of image in the same session. Therefore, XXX_S_Y.bmp means the iris image with index Y in session S from eye XXX.

It is a very crucial task to adopt accurate criterion for any biometric based authentication system. From all the empirical comparison of iris templates computes from the inner right and inner left partial iris image model of eye images available in the CASIA database produced no Hamming distance greater than >0.33 during intra-class comparison and no Hamming distance less than <0.32 during inter-class comparisons respectively. After all this analysis, the Hamming distance was chosen with 0.30 as a criterion or decision threshold (DT) that has produced sustainable performance in the proposed approach. Although comparison results depicted in Figure 4.2 seem to probably show minor FRR (False Reject Rate) occurrence, if 0.30 is considered as a decision threshold (DT) but at the same time is assured not to produce FAR (False Accept Rate). As for the higher security environment is concerned this minor FRR will not affect the performance of the proposed feature extraction method for partial iris image recognition.

Table VII Illustration of a subject iris code (028_1_1) Hamming Distance

Subjects iris	Feature vector (templates) extracted from inner right and inner left partial Iris image model	Dissimilar bits	Hamming Distance (HD)
003_1_1		279	0.52
003_1_2		264	0.49
003_1_3		316	0.59
004_1_2		297	0.55
004_1_3		298	0.55
007_1_2		204	0.38
007_1_2		191	0.35
016_1_3		176	0.33
017_1_1		196	0.36
017_1_2		281	0.52

022_1_2		216	0.40
023_1_3		224	0.41
028_1_1		0	<div data-bbox="886 555 1072 733" style="border: 1px solid black; padding: 5px; display: inline-block;"> Intra-class comparison results for the subject's iris code 028_1_1 </div> <div data-bbox="1096 555 1196 990" style="display: inline-block; vertical-align: middle;"> <div style="border: 1px solid black; border-radius: 50%; padding: 10px; text-align: center;"> 0.00 0.10 0.17 </div> </div>
028_1_2		57	
028_1_3		96	
032_1_1		203	0.38
032_1_2		195	0.36
032_1_3		210	0.39
035_1_1		236	0.43
035_1_2		190	0.35

046_1_2		258	0.48
046_1_3		203	0.38
050_1_2		200	0.37
050_1_3		232	0.42

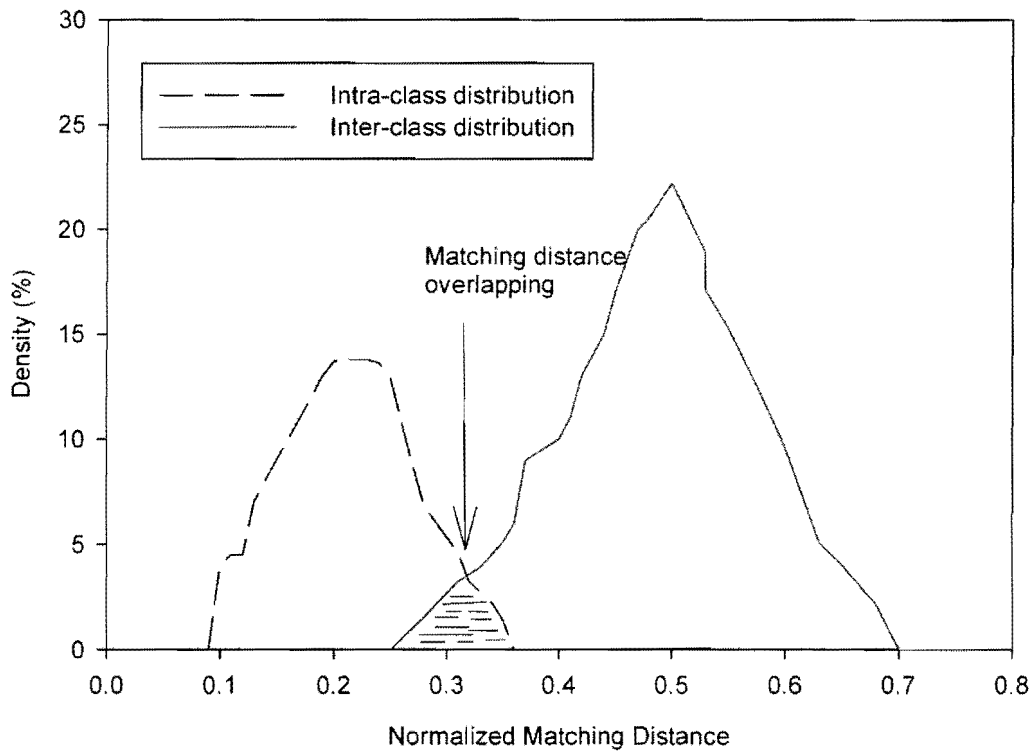


Figure 4.3 Distribution of intra-class and inter-class distances for the templates extracted from the outer right and outer left partial iris image model

The normalized matching distance distribution for the templates generated from the outer right and outer left partial iris image model is illustrated in Figure 4.3. From the Figure 4.3, it is observed that the fractional Hamming distance relies between 0.09 and 0.36 during intra-class or within class comparison whereas the fractional Hamming distances relies between 0.24 and 0.7 during inter-class comparison or unrelated class comparison. As a result, it is observed that normalized matching distance from 0.24 to 0.36 may create uncertainty to making a correct decision since in this case normalized matching score from 0.24 to 0.36 may belong to either in genuine comparison or in the imposter comparison i.e., this region is

overlapped by the both genuine and imposter comparison score. Hence, the intra-class and inter class normalized matching distance shows the features extracted from the outer right and outer left sub image in the outer left and outer right partial iris image model are less discriminant. The outer right and outer left sub image in the outer left and outer right partial iris image model lies closer to the sclera or iris boundary. Ma *et al.* (2004b) and (Xu *et al.*, 2008) found that the iris regions closer to the sclera contains few texture characteristics and are easily occluded by eyelids and eyelashes. Thus, this overlapping may happen due to substantial correlation among the iris features extracted from the outer right and outer left partial iris image model or may increase disagreeing bits among the templates due to noise such as unwrapped partial iris image pattern from the outer right and outer left partial iris image model is occluded by eyelids/eyelashes among different eye images in the database.

Figure 4.3 shows what happens if the criterion point is reduced from 0.30 to 0.24. In this situation, generated feature vector or templates from the outer right and outer left partial iris image model may reduce the false accept rate (FAR) and concurrently increase the false reject rate (FRR). On the contrary, if the criterion point moves from 0.30 to 0.36 that will reduce the false reject rate (FRR) and concurrently increase the false accept rate (FAR) that is a great threat where the high security environment is required. The decision cannot be made without uncertainty when the score is a value between 0.24 and 0.36 and they are both genuine and imposter comparison with values on this range in the distribution functions with the generated features of the outer right and outer left partial iris image model. In that case, when the score belongs to the range of (0.24, 0.36) there is always an existent probability for a mistaken classification that produces lower level of confidence to make a correct decision due to arising overlapping during intra and inter class comparisons.

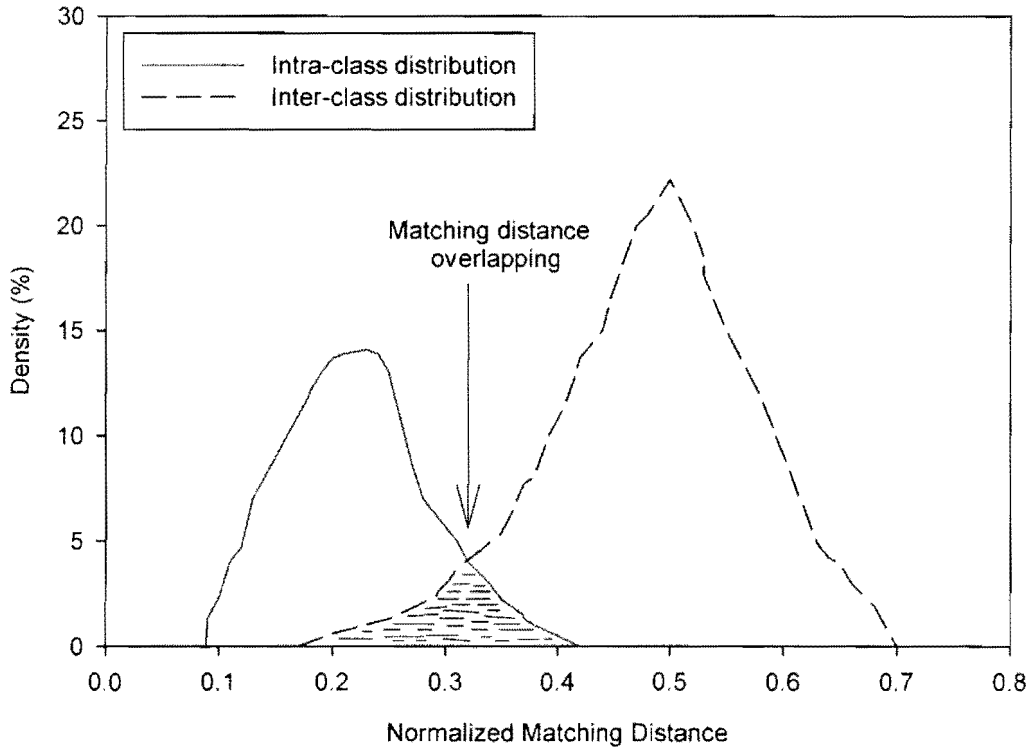


Figure 4.4 Distribution of intra-class and inter-class distances for the templates extracted from the upper and lower partial iris image model.

The normalized intra-class and inter class matching distance distribution of the upper and lower partial iris image models are shown in Figure 4.4. In this case, it is also observed that the normalized matching score relies between 0.09 to 0.43 during intra-class comparison and 0.17 to 0.70 during inter-class comparison respectively. Thus, the correct decision cannot be made while normalized matching score relies from 0.17 to 0.43 since this region may contain overlapping matching score in both intra-class and inter-class comparison. The upper and lower sub image in the upper and lower partial iris image model relies in the collarette boundary which contains more useful and discriminant texture features (Hollingsworth *et al.*, 2008). But, it was detected that the upper and lower sub image in the upper and lower partial

iris image model was occluded by the eyelids and eyelashes in most of the cases during the experiments. This deformation alter the iris features extracted from the upper and lower partial iris image model. This alteration or changes in the features extracted from the upper and lower partial iris image model are caused by occurring false acceptance and false rejection (overlapping matching score) while intra-class and inter-class comparison with the features or templates generated from the upper and lower partial iris image model among the different iris images in the database.

From the analysis of the different kinds of partial iris image models and their comparable experiment result, it is discovered that the proposed feature extraction technique attain promising performance using the features extracted from the inner right and inner left partial iris image model rather than using the features generated from the outer right and outer left, upper and lower partial iris image models respectively. Hence, the inner right and inner left partial iris image model and the features extracted from them have been used to evaluate the performance and accuracy of the proposed feature extraction method for partial iris image recognition.

For a satisfying biometrics algorithm, intra-class distances should hardly vary with time. In this research, the templates extracted from the inner right and inner left partial iris image models have been tested for the eye image taken at different session of the same iris. From the experiment results, it is observed that the intra-class matching distance distribution from comparing images of the same iris taken at the same session is shown in Figure 4.2 and derived from comparing images of the same iris taken at different session is shown in Figure 4.5 are very close. This demonstrates the high stability of the iris features that is extracted from the inner right and inner left partial iris image model. Figure 4.2 and Figure 4.5 also

show that the distance between intra-class and the inter-class distribution is large that indicates the good discriminability of the extracted features from the inner right and inner left partial iris image model. Table VIII depicts the process of intra-class matching distance distribution derived from comparing images of the same iris taken at different session.

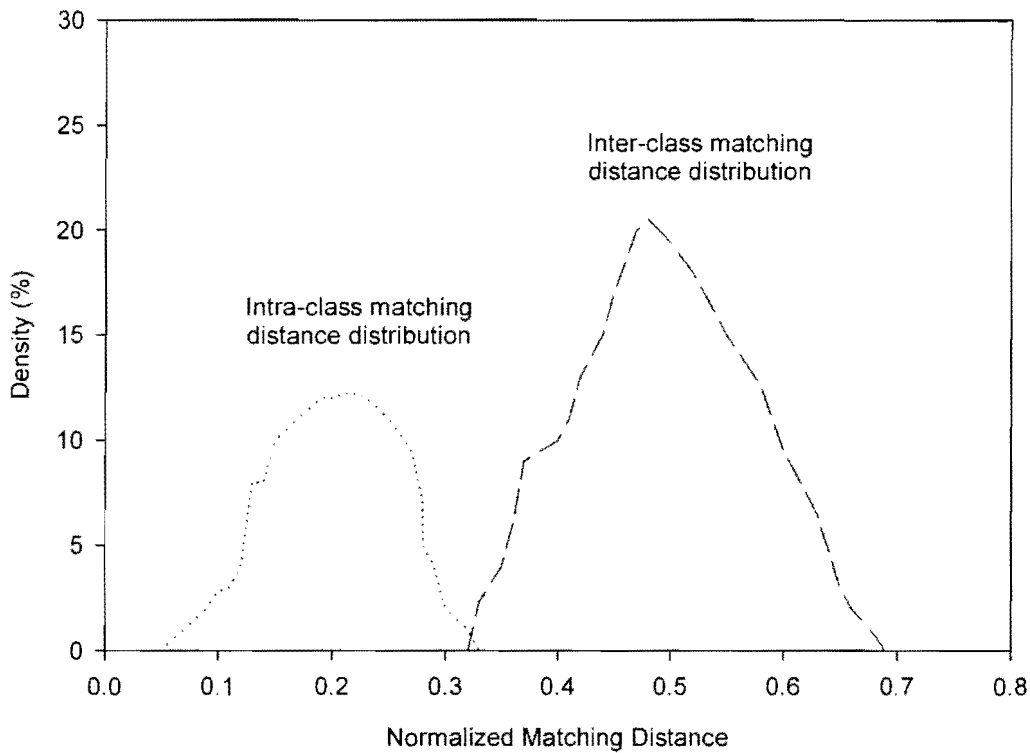






















Figure 4.5 Distribution of intra-class and inter-class distances for the templates extracted from the inner right and inner left partial iris image model from comparing images taken at different session

Table VIII Illustration of subject's iris code (003_1_3, 008_1_3, 014_1_1, 012_1_2, 015_1_2, 018_1_3, 022_1_1, 023_1_3, 026_1_1, 028_1_1, 029_1_1) Hamming Distance

Subjects iris	Feature vector (templates) extracted from inner right and inner left partial iris image model at different session	Dissimilar bits	Hamming Distance (HD)
003_2_1		138	0.25
003_2_2		98	0.18
008_2_1		73	0.13
012_2_1		101	0.18
014_2_1		141	0.26
014_2_2		68	0.12
015_2_1		93	0.17
015_2_2		112	0.20
018_2_1		95	0.17

018_2_2		88	0.16
022_2_2		121	0.22
022_2_3		104	0.19
023_2_1		102	0.18
023_2_4		77	0.14
026_2_1		80	0.14
026_2_3		137	0.25
028_2_1		55	0.10
028_2_2		77	0.14
029_2_1		51	0.09
029_2_2		86	0.15

The observation of the intra-class and inter-class Hamming distance distribution for the three different kinds of partial iris image models shows that the features generated from the inner right and inner left sub image of the collarette boundary of the iris produce stable and discriminant iris texture features among the iris images in the database. The stability of the features generated from the inner right and left partial iris image model is justified by performing intra-class and inter-class comparison of images of the same iris taken at different session. The intra-class matching distance distribution from comparing images of the same iris taken at the same session and derived from comparing images of the same iris taken at different session are very close. This demonstrates the high stability of the iris features extracted from the inner right and inner left partial iris image model. The experimental results also show that the distance between intra-class and the inter-class distribution is large that indicates the good discriminability of the extracted features from the inner right and inner left partial iris image model. The experimental results shows that the features generated from the outer right and outer left sub image provide low discriminant features. Several reasons were detected to occur at low discriminant features generated from outer right and outer left partial iris image model. The outer right and outer left sub image in the outer right and outer left partial iris image model lie closer to the sclera or iris boundary. The iris region closer to the sclera contains few texture characteristics and is easily occluded by eyelids and eyelashes (Ma *et al.*, 2004b; Xu *et al.*, 2008). Thus, the generated features from the outer right and outer left sub image provide low discriminant features due to containing few texture characteristics and occurring noise by occlusion of eyelids and eyelashes. The iris region near to the iris/sclera boundary is corrupted by incorrect outer boundary detection between the iris and sclera especially when there is little contrast between iris and sclera (He & Shi, 2005). This noise also alters the features generated from the outer right and outer left partial iris image model

and hence produces low discriminant features. The upper and lower sub image lays in the collarette boundary of the iris which contains more useful and discriminating texture features (Hollingsworth *et al.*, 2008), although the experiments result show that the discriminant features was not achieved by generating features from the upper and lower partial iris image model. The reasons of this defection was detected that the unwrapped partial upper and lower sub image was corrupted by the noise due to occlusion in most of the cases. These experimental results assert the conjecture that a more distinguishable and individually unique feature is discovered in inner right and inner left sub image of the collarette boundary of the iris and proved the stability of the proposed feature extraction method for partial iris image recognition.

The extensive experiments are also performed in verification mode to measure the accuracy of the proposed method for partial iris image recognition. In verification mode, assuming that a test sample is from a specified subject, and the performance is measured in terms of three error rates: False Acceptance Rate (FAR), False Rejection Rate (FRR) and Equal Error Rate (EER) and these are the most commonly used metrics for a biometric based verification algorithm (Prabhakar *et al.*, 2003; Jain *et al.*, 2004; Anon, 2008). These functions are described in detail in the previous Chapter. Figure 4.6 shows FAR and FRR curve for different threshold values (HD) computed from intra-class and inter-class Hamming distance distribution on Figure 4.2 and 4.5. The False Acceptance Rate (FAR (i)) describes the percent of inter class comparisons with score lower than i and it is interpreted as False Acceptance Rate (FAR) if the value i is selected as DT (Decision Threshold). The False Rejection Rate (FRR (i)) describes the percent of intra-class comparisons with score higher than i and it is interpreted as the False Rejection Rate (FRR) if the value i is selected as DT.

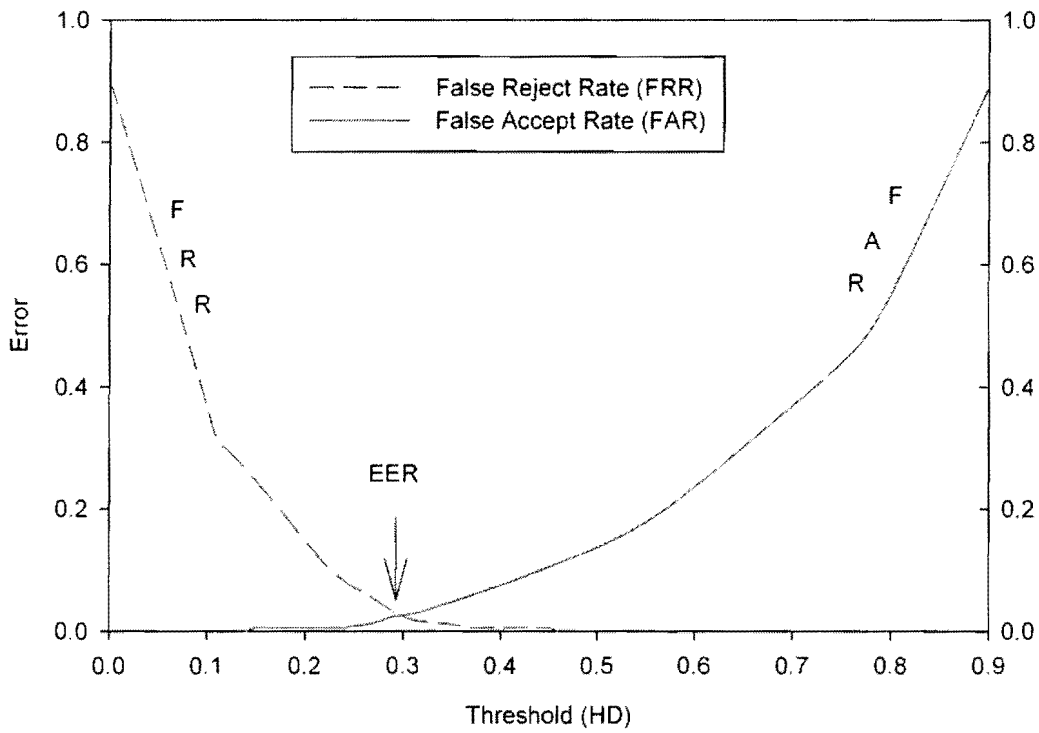


Figure 4.6 FAR and FRR for different threshold (HD) values

From the FAR and FRR curve of the proposed method represents, when the operating criterion (HD) is increased, the probability of a False Accept increases, while that of a False Reject decreases. Instead, as the operating criterion (HD) is decreased, the probability of a False Reject increases and False accept decreases. The EER (Equal Error Rate) occurs at a Hamming distance criterion of about 0.30, at which point both the False Accept Rate and False Reject Rate are equal, 0.28%. The EER is the best single description of the Error Rate of an algorithm and as lower be the EER the lower error rate of the algorithm (Anon, 2008). This EER (Equal Error Rate) suggests adopting a Hamming distance close to 0.30 as a balanced operating criterion in the proposed partial iris image recognition approach. The

accuracy rate of the proposed algorithm is obtained from FAR and FRR which is called Correct Verification Rate (CVR) and calculated as follows:

$$\text{CVR} = (1 - \text{FAR} - \text{FRR}) \times 100\% \quad (4.1)$$

From the FAR and FRR curve in Figure 4.6, the Correct Verification Rate (CVR) obtained 93.27% by our proposed method for partial iris image recognition, where FAR = 3.23% and FRR = 3.5% and HD = 0.30. The proposed approach employed Daubechies DB8 discrete wavelet transform to extract texture features for partial iris image recognition after comparing existing feature extraction techniques although these techniques were used to extract features from the entire iris image. Table IX summarizes the results generated by our approach and the other techniques. These results were published in Masek (2003a) and Roy & Bhattacharya (2008).

Table IX Performance comparisons of several methods for iris verification

Methodology	Correct recognition/verification rate (%)	Number of required bits to store feature vectors	Equal error rate (%)
Lim <i>et al.</i> (2001)	98.4	87	-
Ma <i>et al.</i> (2003)	99.60	1536	.29
Boles & Boashash (1998)	92.64	-	8.13
Poursaberi & Araabi (2007)	97.22 99.31	408 544	1.0334 0.2687
Proposed method (Islam <i>et al.</i> , 2009 ,2010)	93.27	540	.28

From experiments results and analysis discussed above a few conclusions can be made regarding proposed method for partial iris image recognition. Primarily, the proposed feature extraction technique based on Daubechies DB8 discrete wavelet transform can be used efficiently to extract discriminant texture features of the partial iris image for partial iris image recognition. Secondly, the inner right and inner left sub image in the inner right and inner left partial iris image models are discovered as the stable region of the iris and could be used for partial iris recognition system. From the results given in Table VIII, The correct verification rates (CVR) and equal error rate (EER) obtained through the proposed method for partial iris image recognition is comparable to other techniques and only have a slight decrease although these techniques used complete iris for recognition. Note that the results mentioned in the Table VIII in the existing approaches were obtained in the favorable conditions and several research described in the literature review claim that these methods cannot cope with the occlusion problem and thus recognition rate can be deteriorated. Poursaberi *et al.* (2007) proposed two different iris segmentation methods to get rid from the partially occluded iris images so that feature extraction can be done with only iris region. In their first method, they localized collarette boundary of the iris by estimating a certain radius from the edge of the pupil boundary and used the entire collarette boundary of the iris for feature extraction. In their second method, the iris boundary was localized with a large diameter and the lower part of that localized iris was used for feature extraction. They achieved accuracy of 97.22% and 99.31% for their first and second methods respectively as mentioned in the above Table IX. However, they have reported that their methods produce incorrect iris recognition results while collarette region of the iris are occluded. Moreover, the experiment results shown in Figure 4.4 also clarified the fact that using upper and lower

part of the collarette boundary of the iris for recognition are heavily affected by the occlusion of eyelids and eyelashes in most of the cases. The proposed method for partial iris recognition used only two stable regions (inner right and inner left sub image) of the iris to measure accurate verification rate that most of the cases secure from noise and occlusion, and also contains discriminant texture features. The features or templates extracted from the inner right and inner left partial iris image model have been tested for the eye image taken at different session of the same iris in order to justify the stability of the generated features for partial iris recognition. The intra-class and inter-class comparison results and correct verification rate proved the robustness of the proposed method. The unique feature vectors were represented by only 540 bits which minimized the computational time as well.

4.4 Summary

This chapter firstly explained the sample database that was used to evaluate the performance of the proposed feature extraction method for partial iris image recognition. The sample database was collected from The Chinese Academy of Sciences (CASIA) iris image database (CASIA-Iris Image Databases Version 1.0 (CASIA-IrisV1)). Then, the performance evaluation of the proposed feature extraction method has been explained. Firstly, the features were extracted from the inner right and inner left partial iris image model for all of the eye images in the CASIA iris image database. Then, the intra-class and inter-class comparisons were performed in order to observe the matching score behavior based on Hamming distance distribution. The same procedure was followed to observe the intra-class and inter-class matching score behavior for the outer right and outer left, upper and lower partial iris image model. After observing the matching score behavior of the three different kinds of partial iris image models, the more discriminant features and promising performance were achieved

through extracting features of the inner right and inner left partial iris image model. Several reasons of deformation in the features extracted from the outer right and outer left, upper and lower partial iris image models were also explained. Then, the inner right and inner left sub image were detected as the stable region of the iris that could be used for partial iris image recognition. The extracted features of the same iris may change due to the image capturing in different sessions and time. In order to justify of the stability of the features for partial iris image recognition, the intra-class and inter-class comparisons were performed with images of the same iris taken at different session. The comparisons results show that the distance between intra-class and inter-class matching distance distribution was large that indicates the good discriminability of the features extracted from the inner right and inner left partial iris image model. In order to measure the accuracy of the proposed method, the extensive experiments were performed in verification mode and False Accept Rate (FAR), False Reject Rate (FRR), Equal Error Rate was obtained of the proposed method. From the FAR and FRR curve of the proposed method the Correct Verification Rate (CVR) was also calculated. The correct verification rate obtained by the proposed method for partial iris recognition was also compared with the existing methods although these methods used the complete iris for recognition. The correct verification (93.27%) and equal error rate (0.28%) were quite comparable with existing methods and it proves the stability of the proposed feature extraction method based on Daubechies DB8 discrete wavelet transform for partial iris image recognition.

Chapter 5 Conclusion

5.1 Introduction

The focus of this chapter is to discuss the findings of feature extraction method for partial iris image recognition using Daubechies DB8 discrete wavelet transform method. The discussion is based on the results of experiments conducted to evaluate the stability of the features extracted by the proposed feature extraction method. In order to evaluate the stability of the features, partial iris image requirements are also explained in Chapter 3. The three different kinds of partial iris image models are designed based on the review in Chapter 1 and Chapter 2, and observation in the CASIA iris image database. The motivation behind designing the different partial iris image models was to evaluate the stability of the features for partial iris recognition and discovered the stable region on the iris. The main accomplishment of this research is the successful designing and development of the wavelet based feature extraction method for partial iris recognition and derived the stable region of the iris for partial iris recognition.

The main objective of this research study has thus been achieved. The research findings and contributions are discussed in Section 5.2. This research has successfully designed and developed the Daubechies DB8 discrete wavelet transform based feature extraction method for partial iris image recognition that could extract the discriminant texture features from the different high frequency and low frequency band of the wavelet transformed partial iris image.

However, even though the main objective of this research has been achieved the proposed method has some limitations, and a list of future works is discussed to explore the overall solution for partial iris image recognition system.

5.2 Research Findings and Contributions

The main findings and contributions of this research are highlighted in this section. Several achievements of this research are described below.

- The main contribution of this research was to design and develop a feature extraction method in order to extract discriminant texture features for partial iris image recognition using Daubechies DB8 discrete wavelet transform method.
- The inner right and inner left sub image in the collarette boundary of the iris have been discovered as the stable region of the iris that could be used for partial iris image recognition efficiently.
- This research also proposed a computationally efficient feature vector with as few as possible number of features which is comprised with only 540 bits.

The previous research in iris recognition may produce false result due to incomplete iris image during identification or verification. The previous feature extraction techniques for iris image recognition used complete iris for feature extraction and stored extracted features as a unique feature vector in the database during enrollment. But, it is observed that unfortunately $\frac{1}{3}$ of the complete iris is obstructed in most cases during verification/identification due to partially occluded by interference of eyelids and some part of the iris is often covered by eyelashes, improper eye openings and other extraneous artifice. Hence, the previous research fail to correctly verify or identify of an individual due to loss of abundant iris characteristics

features as compared to once enrolled feature vector of the individual. This observation motivated us to design and developed a feature extraction method to extract discriminant texture features of the partial iris image in order to identify an individual by their only significant part of the iris for partial iris image recognition.

Several feature extraction techniques in the previous research has been studied and analyzed although these methods used the entire iris to extract unique features. From the analysis of the previous feature extraction techniques, it was observed that these techniques may not be fit to extract unique features of the partial iris image for partial iris recognition. Several problems of the existing feature extraction techniques to utilize to extract features of the partial iris image are addressed in Chapter 2 and in Chapter 3.

Based on these problems, this research contributes to the design and development of a feature extraction method to extract discriminant texture features of the partial iris image using Daubechies DB8 discrete wavelet transform, and it is a kind of technique analysing signals in multi-resolution mode. When processing signals, the primary consideration is the localization, i.e., the characterization of local properties of a given basis function in time and frequency. The Gabor transform and Haar wavelet transform are widely used in the iris feature analysis. However, the outputs of Gabor filter banks are not mutually orthogonal, which may result in a significant correlation between texture features. Another weakness of the Gabor filter in which the even symmetric filter will have a DC component whenever the bandwidth is larger than one octave that means DC component may affect of the computed iris code by the strength of illumination due to DC response in real parts of the filtered image. The characteristics vectors generated by these methods are formed to have 256 or more dimensions, and they require at least 256 bytes even though it is assumed that one byte is

assigned to one dimension. There are problems with Haar's construction. For example, Haar's base functions are discontinuous step functions and are not suitable for analyzing continuous functions with continuous derivatives. If images are considered as 2-D continuous surfaces, the Haar's base functions are not appropriate for image analysis. On the contrary, the Daubechies wavelet functions are continuous functions. The disadvantages of Haar wavelet functions that the values thereof discontinuous and rapidly changes can be avoided, and the characteristics values can be extracted more accurately. Therefore, in case where the images are to be again decompressed after they have been compressed by using the Daubechies wavelet transform, the images can be restored in high resolution nearer to the original images than the Haar wavelet transform is used. The Daubechies wavelet transform also reduces the dimension of the characteristics vector. The Daubechies DB8 discrete wavelet transform was repeatedly applied to the unwrapped normalized partial iris image in order to extract the discriminant texture features. Then, the only high frequency components at the fourth level of wavelet transformed image were selected as unique features. Spatial information is of critical importance in high frequency bands than that of lower frequency bands. This is because high frequencies mostly occur for a shorter span than that of low frequencies. Thus, the high frequency components of the partial iris image gives better discrimination among the templates extracted from the different iris images in the database. This feature extraction technique also contributes by introducing a discriminant feature vector with as few as possible number of features which is comprised with only 540 bits whereas the feature vector of the previous research is very large as many as 1024 bits where the higher computations and space is required to process and store these iris features.

This research also contributes by identifying the stable region or significant part of the iris that could be used for partial iris image recognition. The three different kinds of partial iris

image models were designed in order to evaluate the stability of the texture features extracted through the proposed feature extraction technique of the partial iris image. The intra-class and inter-class comparisons were done based on Hamming distance by extracting features through different kinds of partial iris image models. From the analysis of comparison results, the better discrimination was achieved with templates extracted from the inner right and inner left partial iris image model. The comparisons results with the templates extracted from the upper and lower, outer right and left partial iris image model were always remained as possible occurrence for false accept and false reject. Finally, the intra-class and inter-class comparison results with the templates generated from the inner right and inner left sub image model have been utilized to measure the accuracy of the proposed method. The verification results showed that this research produce $FAR = 3.23\%$ and $FRR = 3.5\%$ and low EER (0.28%). The accuracy more than 90% was achieved during verification with the templates extracted from the inner right and inner left partial iris image. These results proved the stability of the proposed method to extract texture features and inner right and inner left sub image in the collarette boundary of the iris as stable region for partial iris image recognition.

As a conclusion for the findings and contribution of this research, the most significant contribution of this research is to introduce a new feature extraction method based on Daubechies DB8 discrete wavelet transform to extract distinctive texture features for partial iris recognition. The proposed method also contributes by generating unique feature vectors with low number of feature components which is comprised with only 540 bits. Moreover, this research also contributes by identifying the stable region or significant part of the iris that could be used for partial iris image recognition.

5.3 Limitations

The proposed feature extraction method and stable region determination technique for partial iris image recognition have some limitations. The first one relates to the features that have been extracted for partial iris image recognition. The texture features of the partial iris image were extracted only from the high frequency component of the Daubechies DB8 wavelet transformed image. The texture regions of the partial iris image has higher frequency components and gives better discriminant features than the low frequency components of the decomposed partial iris image. But, the limitation of this technique is that the high frequency component of the wavelet transformed image is noise sensitive. The collarette region of the iris contains most of discriminating texture patterns. The upper and lower sub image region in the upper and lower partial iris image model rely on the collarette boundary of the iris. Although the overlapping of intra-class and inter-class Hamming distance distribution of the upper and lower partial iris image model showed that the extracted texture features only from the high frequency components are noise sensitive since the upper and lower sub image region in the upper and lower partial iris image model is affected by noise such as occlusion of eyelids and eyelashes.

5.4 Future Works

After reviewing the findings and the limitation of this research, there are a number of areas where future research can be done to further improve the feature selection process and the stable region determination mechanism so that they can be employed to a wider range of partial iris verification system.

In this research, the three partial iris image models are designed. The Daubechies DB8 discrete wavelet transform was applied to the partial iris images to extract unique texture features. Then, the only high frequency components and their variances of the last level of wavelet transformed image were selected as unique texture features for the three different kinds of partial iris image models separately. The intra-class and inter-class comparisons were performed based on Hamming distance with extracting feature vector from the three kinds of partial iris image models separately. The promising results were achieved with the feature vector generated from the inner right and inner left partial iris image model and it was selected as a stable region of the iris to be used for partial iris recognition and justified the stability of the features.

Partial iris image recognition research is new and it requires extensive the analysis on more features that can be contributed to the list of features to be selected to ensure the features selected are at the most optimum. In this consequence, the importance of extension of this research will be to select few of the low frequency component and their variances of the different level of low frequency band of the wavelet transformed image and combine with the high frequency component in order to make a discriminant feature vector of the partial iris image.

Another important further extension of this research will be to select only discriminant and noise free texture features of the outer right and outer left, upper and lower partial iris image model separately and integrate it with the extracted distinctive texture features of the inner right and inner left partial iris image model in order to make a discriminant feature vector of the partial iris image for partial iris image recognition.

The feature vector with 540 bits was generated to represent partial iris image in this research. The Hamming distance similarity measurement technique was used for intra-class and inter-class comparison. The Hamming distance is also excellent for application with the extracted iris features by subdividing the data, but it may not produce the best result when low capacity data is to be used. Therefore, future research should be done in order to find out a similarity measurement technique for handling low capacity feature vectors that would be able to classify among related and unrelated feature vectors with high level of confidence.

5.5 Conclusion

The feature extraction method to extract discriminant texture features and discovering the stable regions of the iris for partial iris recognition have been accomplished successfully. This approach used Daubechies discrete wavelet transform with eight coefficients in order to extract iris texture features which are easy to compute and interpret. The Daubechies DB8 wavelet transform is faster compared to other methods on texture analysis. Daubechies DB8 wavelet transform allows keeping the feature vectors into significantly lesser number of bits without affecting the accuracy of the result. The generated feature vector of the inner right and inner left partial iris image model were comprised of only 540 bits which minimized the overall processing time of partial iris recognition system. The experiments were performed with the different kinds partial iris image models selected from the different location of the iris in order to discover the stable region of the iris and to evaluate the stability of proposed feature extraction method to extract distinctive texture features of the iris for partial iris image recognition. The promising results were achieved with the templates or feature vectors extracted from the inner right and inner left partial iris image model. More than 90% accuracy was achieved during partial iris image verification with the templates or feature vectors

extracted from the inner right and inner left partial iris image model. These experiments results assert the stability of the proposed feature extraction method for partial iris image recognition. The process of evaluating of the new feature extraction method for partial iris recognition not only shows the extracted features for partial iris recognition but also derive the stable region of the iris that could be used for partial iris recognition. The experiments results show that most discriminating and severally unique patterns appeared in collarette boundary of the iris. Despite the limitations, the experiments results show that the proposed feature extraction method of the partial iris image is able to overcome the problem when false results occur due partially occluded of iris images in the existing approaches. However, the experiment results also show that a partial iris image can be used for human identification/verification. Undoubtedly, improvement could be done with more extensive analysis, hypothesis and implementation in the future.

Bibliography

Adler, F. H. (1965). *Physiology of the eye* (4th ed.). St. Louis, MO: Mosby.

Ali, J. M., & Hassanien, A. E. (2003). An iris recognition system to enhance e-security environment based on wavelet theory. *Advanced Modelling and Optimization (AMO)* , 5 (2), 93-104.

Annappoorani, G., Krishnamoorthi, R., Jeya, P. G., & Petchiammal@Sudha, S. (2010). Accurate and fast iris segmentation. *International Journal of Engineering Science and Technology* , 2 (6), 1492-1499.

Anon. (2006). *Iris recognition*. Retrieved 2009, from National Science and Technology Council (NSTC): <http://www.biometrics.gov/Documents/irisrec.pdf>

Anon. (2008). *Understanding biometrics*. Retrieved 2009, from Griaule Biometrics: <http://www.griaulebiometrics.com/page/en-us/book/understanding-biometrics>

Arivazhagan, S., & Ganesan, L. (2004). Automatic target detection using wavelet transform. *EURASIP Journal on Applied Signal Processing* , 2004 (17), 2663-2674.

Basit, A., & Javed, M. Y. (2007). Localization of iris in gray scale images using intensity gradient. *Optics and Lasers in Engineering* , 45 (12), 1107-1114.

Boles, W. W., & Boashash, B. (1998). A human identification technique using images of the iris and wavelet transform. *IEEE Transaction on Signal Processing* , 46 (4), 1185-1188.

Bowyer, K. W., Hollingsworth, K., & Flynn, P. J. (2008). Image understanding for iris biometrics: a survey. *Computer Vision and Image Understanding* , 110 (2), 281-307.

Bremananth, R., & Chitra, A. (2008). Rotation invariant recognition of iris. *Journal of Systems Science and Engineering* , 17 (1), 69-78.

CASIA-Iris Image Databases Version 1.0 (CASIA-IrisV1). (n.d.). Retrieved 2008, from Biometrics ideal test: <http://biometrics.idealtest.org/>

Cha, S. -H., Tappert, C., & Yoon, S. (2006). Enhancing binary feature vector similarity measures. *Journal of Pattern Recognition Research* , 1 (1), 63-77.

Chang, T., & Kuo, C.-C. J. (1993). Texture analysis and classification with tree-structured wavelet transform. *IEEE Transaction on Image Processing* , 2 (4), 429-441.

Chen, W. S., Huang, R. H., & Hsieh, L. (2009). Iris recognition using 3D co-occurrence matrix. *In Proceedings of the 3rd International Conference on Advances in Biometrics (ICB)*, (pp. 1122-1131).

Daubechies, I. (1988). Orthonormal bases of compactly supported wavelets. *Communications on Pure and Applied Mathematics* , 41 (7), 909-996.

Daubecheis, I. (1992). *Ten Lectures on Wavelets*. Philadelphia, PA, USA: Society for Industrial and Applied Mathematics.

Daugman, J. (University of Cambridge). *Evolving methods in iris recognition*. Retrieved 2009, from http://www.cse.nd.edu/BTAS_07/John_Daugman_BTAS.pdf

Daugman, J. (1993). High confidence visual recognition of persons by a test of statistical independence. *IEEE Transaction on Pattern Analysis and Machine Intelligence* , 15 (11), 1148-1161.

Daugman, J. G. (1994). *Patent No. 5,291,560*. U. S.

Daugman, J. (2001a). Iris recognition. *American Scientist* , 89, pp. 326-333.

Daugman, J. (2001b). High confidence recognition of persons by iris patterns. *2001 IEEE 35th International Carnahan Conference on Security Technology*, (pp. 254-263).

Daugman, J. (2003). The importance of being random: statistical principles of iris recognition. *Pattern Recognition* , 36 (2), 279-291.

- Daugman, J. (2004). How iris recognition works. *IEEE Transactions on Circuits and Systems for Video Technology* , 14 (1), 21-30.
- Dey, S., & Samanta, D. (2008). A novel approach to iris localization for iris biometric processing. *International Journal of Biological and Life Sciences* , 3 (3), 180-191.
- Dong, W., Sun, Z., Tan, T., & Wei, Z. (2009). Quality-based dynamic threshold for iris matching. *IEEE International Conference on Image Processing*, (pp. 1949-1952).
- Dorairaj, V., Schmid, N. A., & Fahmy, G. (2005). Performance evaluation of non-ideal iris based recognition system implementing global ICA encoding. *IEEE International Conference on Image Processing*, (pp. 285-288).
- Field, D. J. (1987). Relations between the statistics of natural images and the response properties of cortical cells. *Journal of Opt. Soc. Am. A* , 4, 2379-2394.
- Flom, L., & Safir, A. (1987). *Patent No. 4,641,349*. U.S.
- Gawande, U., Zaveri, M., & Kapur, A. (2010). Improving iris recognition accuracy by score based fusion method. *International Journal of Advancements in Technology (IJoAT)* , 1 (1).
- Gopikrishnan, M., & Santhanam, T. (2010). Neural network based accurate biometric recognition and identification of human iris patterns. *Journal of Computer Science* , 6 (10), 1170-1173.
- He, X., & Shi, P. (2005). An efficient iris segmentation method for recognition. *Pattern Recognition and Image Analysis* , 3687, 120-126.
- Hollingsworth, K., Bowyer, K., & Flynn, P. (2008). The best bits in an iris code. *IEEE Transaction on Pattern Analysis and machine Intelligence* , 31 (6), 963-973.
- Hollingsworth, K. P., Bowyer, K. W., & Flynn, P. J. (2009). Image averaging for improved iris recognition. *In proceeding of the 3rd International Conference on Advances in Biometrics (ICB)*, (pp. 1112-1121).

- Islam, M. R., Wang, Y. C., & Khatun, A. (2009). A wavelet transform feature processing approach for partial iris image recognition. *In proceedings of the First Malaysian Joint Conference on Artificial Intelligence (MJCAI)*. Kuala Lumpur, Malaysia.
- Islam, M. R., Wang, Y. C., & Khatun, A. (2010). Partial iris image recognition using wavelet based texture features. *In IEEE Proceedings of the 3rd International Conference on Intelligent & Advanced Systems (ICIAS2010)*. Kuala Lumpur Convention Centre, Malaysia.
- Jain, A. K., Ross, A., & Prabhakar, S. (2004). An introduction to biometric recognition. *IEEE Transactions on Circuits and Systems for Video Technology* , 14 (1), 4-20.
- Kim, J., Cho, S., Choi, J., & Marks II, R. J. (2004). Iris recognition using wavelet features. *VLSI Signal Processing* , 38 (2), 147-156.
- Kim, J., Cho, S., Kim, D., & Chung, S. -T. (2006). Iris recognition using a low level of details. *In Advances in Visual Computing* (Vol. 4292/2006, pp. 196-204). USA: Springer Berlin / Heidelberg.
- Ko, J. -G., Gil, Y. -H., Yoo, J. -H., & Chung, K. -I. (2007). A novel and efficient feature extraction method for iris recognition. *ETRI Journal* , 29 (3), 399-401.
- Lakshmi, A., & Rakshit, S. (2010). New wavelet features for image indexing and retrieval. *2nd IEEE International Conference on Advance Computing Conference (IACC)*, (pp. 145-150).
- Lim, S., Lee, K., Byeon, O., & Kim, T. (2001). Efficient iris recognition through improvement of feature vector and classifier. *ETRI Journal* , 23 (2), 61-70.
- Ma, L., Tan, T., Wang, Y., & Zhang, D. (2003). Personal identification based on iris texture analysis. *IEEE Transaction on Pattern Analysis and Machine Intelligence* , 25 (12), 1519-1533.
- Ma, L., Tan, T., Zhang, D., & Wang, Y. (2004a). Local intensity variation analysis for iris recognition. *Pattern Recognition* , 37 (6), 1287-1298.

- Ma, L., Tan, T., Wang, Y., & Zhang, D. (2004b). Efficient iris recognition by characterizing key local variations. *IEEE Transactions on Image Processing* , 13 (6), 739–750.
- Ma, Z., Qi, M., Kang, H., Wang, S., & Kong, J. (2007). Iris verification using wavelet moments and neural network. In *Life System Modeling and Simulation* (Vol. 4689/2007, pp. 218-226). Shanghai, China: Springer Berlin / Heidelberg.
- Mallat, S. G. (1989). A theory for multiresolution signal decomposition: the wavelet representation. *IEEE Transaction on Pattern Analysis and Machine Intelligence* , 11 (7), 674-693.
- Mallat, S., & Hwang, W. (1992). Singularity detection and processing with wavelets. *IEEE Transaction on Information Theory* , 38 (2), 617-643.
- Mallat, S. G. (1998). *A wavelet tour of signal processing*. Academic Press.
- Manjunath, A., & Ravikumar, H. M. (2010). Comparison of discrete wavelet transform (DWT), lifting wavelet transform (LWT) stationary wavelet transform (SWT) and s-transform in power quality analysis. *European Journal of Scientific Research* , 39 (4), 569-576.
- Masek, L. (2003a). *Recognition of human iris patterns for biometric identification*. University of Western Australia, Perth, Australia.
- Masek, L., & Kovesi, P. (2003b). *MATLAB source code for a biometric identification system based on iris patterns*. Retrieved from University of Western Australia: <http://people.csse.uwa.edu.au/pk/studentprojects/libor/>
- Min, T. -H., & Park, R. -H. (2009). Eyelid and eyelash detection method in the normalized iris image using the parabolic hough model and otsu's thresholding method. *Pattern Recognition Letters* , 30 (12), 1138-1143.

Munemoto, T., Hui, L. -Y., & Savvides, M. (2008). Hallucinating irises-dealing with partial and occluded iris regions. *2nd IEEE international conference on Biometrics: Theory, Applications, and Systems*, (pp. 1-6).

(n.d.). Retrieved from Multimedia University Iris Image Database: <http://pesona.mmu.edu.my/ccte/>

Poursaberi, A., & Araabi, N. B. (2007). Iris recognition for partially occluded images: methodology and sensitivity analysis. *EURASIP Journal on Advances in Signal Processing*, vol. 2007, 12 pages.

Prabhakar, S., Pankanti, S., & Jain, A. K. (2003). Biometric recognition: security and privacy concerns. *IEEE Security & Privacy*, 1 (2), 33-42.

Roy, K., & Bhattacharya, P. (2008). Optimal features subset selection and classification for iris recognition. *EURASIP Journal on Image and Video Processing*, 2008, 20 pages.

Sivabalan, K. N., & Ghanadurai, D. (2010). Detection of defects in digital texture images using segmentation. *International Journal of Engineering Science and Technology*, 2 (10), 5187-5191.

Sun, Z., & Tan, T. (2009). Ordinal measures for iris recognition. *IEEE Transaction on Pattern Analysis and Machine Intelligence*, 31(12), 2211-2226.

Tajbakhsh, N., Araabi, B. N., & Zadeh, H. S. (2010). Robust iris verification based on local and global variations. *EURASIP Journal on Advances in Signal Processing*, 2010, 12 pages.

Tang, R., Han, J., & Zhang, X. (2009). Efficient iris segmentation method with support vector domain description. *Optica Applicata*, 39 (2), 365-374.

(2005). *The LSE identity project interim report: an assessment of the UK identity cards bill and its implications*. London: The London School of Economics & Political Science, The Department of Information System.

Thuillard, M. (2001). Wavelets in soft computing. In *Worlds scientific series in Robotics and Intelligent Systems* (Vol. 25, p. 248 pages). Switzerland: (Siemens Building Technologies).

Tisse, C., Martin, L., Torres, L., & Robert, M. (2002). Person identification technique using human iris recognition. In *Proceedings of the 15th International Conference on Vision Interface (VI)*, (pp. 294-299). Calgary, Canada.

University of Bath Iris Image Database. (2007). Retrieved from <http://www.bath.ac.uk/elect-eng/research/sipg/irisw/>

Unser, M. (1995). Texture classification and segmentation using wavelet frames. *IEEE Transaction on Image Processing* , 4 (11), 1549-1560.

Vasta, M., Singh, R., & Noore, A. (2005). Reducing the false rejection rate of iris recognition using textural and topological features. *International Journal of Signal Processing* , 2 (2), 66-72.

Vetterli, M., & Herley, C. (1992). Wavelets and filter banks: theory and design. *IEEE Transaction on Signal processing* , 40 (9), 2207-2232.

Wang, J. Z., Wiederhold, G., Firschein, O., & Wei, S. X. (1998). Content-based image indexing and searching using daubechies wavelets. *International Journal on digital Libraries* , 1 (4), 311-328.

Wei, Z., Tan, T., Sun, Z., & Cui, J. (2005). Robust and fast assessment of iris image quality. In *Advances in Biometrics* (Vol. 3832/2005, pp. 464-471). China: Springer Berlin / Heidelberg.

Wildes, R. P. (1997). Iris recognition: an emerging biometric technology. In *Proceedings of the IEEE*, 85(9), pp. 1348-1363.

Wildes, R. P., Asmuth, J. C., Green, G. L., Hsu, S. C., Kolczynski, R. J., Matey, J. R., et al. (1996). A machine-vision system for iris recognition. *Machine Vision and Application* , 9, 1-8.

Wouwer, G. V., Scheunders, P., & Dyck, D. V. (1999). Statistical texture characterization from discrete wavelet representations. *IEEE Transaction on Image Processing* , 8, 592-598.

Xu, G., Zhang, Z., & Ma, Y. (2006). Automatic iris segmentation based on local areas. *18th International Conference on Pattern Recognition (ICPR'06), Vol. 4*, (pp. 505-508).

- Xu, G., Zhang, Z., & Ma, Y. (2008). A novel method for iris feature extraction based on intersecting cortical model network. *Journal of Applied mathematics and Computing* , 26 (1-2), 341-352.
- Yahya, A. E., & Nordin, M. J. (2010). Accurate iris segmentation method for non-cooperative iris recognition system. *Journal of Computer Science* , 6 (5), 527-532.
- Zhu, Y., Tan, T., & Wang, Y. (2000). Biometric personal identification based on iris patterns. *In Proceedings of the 15th International Conference on Pattern Recognition*, 2, pp. 801-804.
- Zuiderveld, K. (1994). *Contrast limited adaptive histogram equalization*. San Diego, CA, USA: Academic Press Professional, Inc.

Appendix I

Hough Transform

The Hough transform is a standard computer vision algorithm that can be used to determine the parameters of simple geometric objects, such as lines and circles, present in an image. The circular Hough transform can be employed to deduce the radius and centre coordinates of the pupil and iris regions. An automatic segmentation algorithm based on the circular Hough transform is employed by Wildes (1997) and Wildes *et al.* (1996). In the proposed method by Wildes, an edge map of the image is first obtained by thresholding the magnitude of the image intensity gradient:

$$|\nabla G(x, y) * I(x, y)|,$$

where, $\nabla \equiv (\delta / \delta x, \delta / \delta y)$ and $G(x, y) = \frac{1}{2\pi\sigma^2} e^{-\frac{(x-x_0)^2 + (y-y_0)^2}{2\sigma^2}}$. $G(x, y)$ is a Gaussian smoothing function with scaling parameter σ to select the proper scale of edge analysis.

The edge map is then used in a voting process to maximize the defined Hough transform for the desired contour. Considering the obtained edge points as (x_j, y_j) , $j = 1, 2, \dots, n$, a Hough transform can be written as:

$$H(x_c, y_c, r) = \sum_{j=1}^n h(x_j, y_j, x_c, y_c, r),$$

$$\text{where, } h(x_j, y_j, x_c, y_c, r) = \begin{cases} 1 & \text{if } g(x_j, y_j, x_c, y_c, r) = 0; \\ 0 & \text{otherwise.} \end{cases}$$

The limbus and pupil are both modelled as circles and the parametric function g is defined as:

$$g(x_j, y_j, x_c, y_c, r) = (x_j - x_c)^2 + (y_j - y_c)^2 - r^2$$

Assuming a circle with the center (x_c, y_c) and radius r , the edge points that are located over the circle result in a zero value of the function. The value of g is then transformed to 1 by the h function, which represents the local pattern of the contour. The local patterns are then used in a voting procedure using the Hough transform, H , in order to locate the proper pupil and limbus boundaries. In order to detect limbus, only vertical edge information is used. The upper and lower parts, which have the horizontal edge information, are usually covered by the two eyelids. The horizontal edge information is used for detecting the upper and lower eyelids, which are modeled as parabolic arcs.